Title

Chronic alcohol disrupts hypothalamic responses to stress by modifying CRF and NMDA receptor function

Authors

Marty, Vincent N
Mulpuri, Yatendra
Munier, Joseph J
et al.

Publication Date

2020-05-01

DOI

10.1016/j.neuropharm.2020.107991

Peer reviewed

HHS Public Access

Author manuscript

Neuropharmacology. Author manuscript; available in PMC 2021 May 01.

Published in final edited form as:

Neuropharmacology. 2020 May 01; 167: 107991. doi:10.1016/j.neuropharm.2020.107991.

Chronic alcohol disrupts hypothalamic responses to stress by modifying CRF and NMDA receptor function

Vincent N. Marty[1,*], **Yatendra Mulpuri**[1], **Joseph J. Munier**[1], **Igor Spigelman**[1,2]

[1]Laboratory of Neuropharmacology, Section of Oral Biology, School of Dentistry, Los Angeles, CA, 90095-1668. USA

[2]Brain Research Institute, University of California, Los Angeles, CA, 90095-1668. USA

Abstract

The chronic inability of alcoholics to effectively cope with relapse-inducing stressors has been linked to dysregulation of the hypothalamic-pituitary-adrenal (HPA) axis and corticotropin-releasing factor (CRF) signaling. However, the cellular mechanisms responsible for this dysregulation are yet to be identified. After exposure of male Sprague Dawley rats to chronic intermittent ethanol (CIE; 5–6g/kg orally for 35 doses over 50 days) or water, followed by 40–60 days of protracted withdrawal, we investigated CIE effects on glutamatergic synaptic transmission, stress-induced plasticity, CRF- and ethanol-induced NMDAR inhibition using electrophysiological recordings in parvocellular neurosecretory cells (PNCs) of the paraventricular nucleus. We also assessed CIE effects on hypothalamic mRNA expression of CRF-related genes using real-time polymerase chain reaction, and on HPA axis function by measuring stress-induced increases in plasma adrenocorticotropic hormone, corticosterone, and self-grooming. In control rats, ethanol-mediated inhibition of NMDARs was prevented by CRF1 receptor (CRFR1) blockade with antalarmin, while CRF/CRFR1-mediated NMDAR blockade was prevented by intracellularly-applied inhibitor of phosphatases PP1/PP2A, okadaic acid, but not the selective striatal-enriched tyrosine protein phosphatase inhibitor, TC-2153. CIE exposure increased GluN2B subunit-dependent NMDAR function of PNCs. This was associated with the loss of both ethanol- and CRF-mediated NMDAR inhibition, and loss of stress-induced short-term potentiation of glutamatergic synaptic inputs, which could be reversed by intracellular blockade of NMDARs with MK801. CIE exposure also blunted the hormonal and self-grooming behavioral responses to repeated restraint stress. These findings suggest a cellular mechanism whereby chronic alcohol

[*]Corresponding author with complete address, including an email address and postal code: Dr. Vincent N. Marty, UCLA School of Dentistry, 10833 Le Conte Avenue, 63-078 CHS, Los Angeles, CA 90095-1668, (310) 825-6509, vincentmarty@g.ucla.edu, martyv@ymail.com.

Credit Author Statement

Vincent N. Marty: Conceptualization, Methodology, Validation, Formal Analysis, Investigation, Writing – Original Draft, Visualization, Funding Acquisition. **Yatendra Mulpuri**: Conceptualization, Methodology, Validation, Investigation, Writing – Review & Editing. **Joseph J. Munier**: Conceptualization, Methodology, Investigation, Writing – Review & Editing, Funding Acquisition. **Igor Spigelman**: Conceptualization, Methodology, Investigation, Writing – Review & Editing, Supervision, Project Administration, Funding Acquisition.

dysregulates the hormonal and behavioral responses to repetitive stressors by increasing NMDAR function and decreasing CRFR1 function.

Graphical Abstract

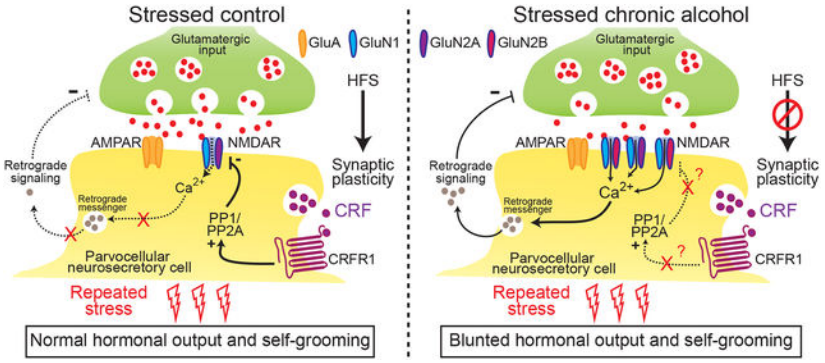

1. INTRODUCTION

Alcohol use disorder (AUD) is associated with persistent maladaptive changes of the hypothalamic-pituitary-adrenal (HPA) axis leading to altered responses to stress and increased susceptibility to stress-induced negative emotions. Chronic alcohol (ethanol) exposure produces persistent reorganization in brain function which defines a new equilibrium around a new ‘set-point’, termed allostasis (Koob, 2003; Le Moal, 2009). These allostatic changes contribute to alcohol craving and relapse during protracted abstinence (Adinoff et al., 2005; Heilig and Koob, 2007; Huang et al., 2010; Koob, 2008; Lee et al., 2011; Li et al., 2011; Overstreet et al., 2004; Pohorecky, 1991; Sinha et al., 2009; Sinha et al., 2011). Normally, stress activates the HPA axis producing an appropriate physiological response to meet the impending challenge. The parvocellular neurosecretory cells (PNCs) in the paraventricular nucleus of the hypothalamus (PVN) represent the central integrative and penultimate step of the HPA axis response to stressors (Bains et al., 2015; Herman et al., 2002), whereby activation causes release of corticotropin-releasing factor (CRF) and subsequent elevations in circulating adrenocorticotropic hormone (ACTH) and adrenal glucocorticoids such as corticosterone (CORT). The effects of CRF and structurally related urocortin peptides are mediated by two G-protein-coupled receptors subtypes (CRFR1 and CRFR2) and modulated by CRF-binding protein (Bale and Vale, 2004).

Activation of CRFR1 and CRFR2 affects cyclic AMP/protein kinase A (cAMP/PKA)-meditated modulation of protein kinases and phosphatases, such as PP1 and PP2A, which in turn regulates the phosphorylation state of various receptors, including AMPAR and NMDAR (Leslie and Nairn, 2019). CRFRs can also interact with a variety of G-protein coupled systems activating a multitude of different intracellular pathways mediating different CRF effects depending on their localization and cellular context. For example, CRF-induced potentiation of NMDARs requires cAMP/PKA pathways in central amygdala (Fu and Neugebauer, 2008; Ji et al., 2013), and phospholipase C/protein kinase C (PLC/PKC) in the VTA (Ungless et al., 2003), while in the hippocampus, CRF-induced depression

of NMDARs involves the activation of PLC/inositol-1,4,5-triphosphate receptor and PLC/PKC pathways (Sheng et al., 2008).

Stress unmasks multiple types of adaptive synaptic plasticity, or metaplasticity, in PNCs (Hewitt et al., 2009; Inoue et al., 2013; Kusek et al., 2013; Kuzmiski et al., 2010; Sarkar et al., 2011; Wamsteeker et al., 2010). For instance, acute restraint stress induces a CRF/CRFR1-dependent depression of NMDAR function at glutamatergic synapses of CRF-expressing PNCs, which allows for short-term synaptic potentiation (STP) of AMPAR-mediated excitatory postsynaptic currents following a burst of high-frequency stimulation (HFS) of afferent inputs (Kuzmiski et al., 2010; Sterley et al., 2018). This STP requires CRF-mediated decreases in postsynaptic NMDAR-dependent Ca^{2+} entry to prevent the release of a postsynaptic retrograde messenger that normally restrains presynaptic glutamate release (Kuzmiski et al., 2010). Although the precise physiological significance of stress-induced STP following HFS is unknown, it is hypothesized to be critical for the integration and processing of the HPA axis' adaptive responses to stressors (Bains et al., 2015; Marty et al., 2011; Ramot et al., 2017; Sterley et al., 2018). Stress-induced STP in PNCs was recently reported to be necessary for release of a putative alarm pheromone transmitting distress signals to conspecific subjects (Sterley et al., 2018). It was also shown that glutamatergic neurotransmission of CRF-expressing PNCs within the PVN is essential in regulating a complex repertoire of stress-induced coping behaviors, including self-grooming (Füzesi et al., 2016). Thus, dysregulation of stress-induced synaptic plasticity of PNCs could lead to maladaptive hormonal and behavioral responses to stress.

Acutely, ethanol exposure up-regulates CRF mRNA levels within the PVN and increases plasma ACTH levels via a PVN CRF-dependent mechanism (Lee et al., 2004; Rivest and Rivier, 1994). Chronic ethanol exposure induces persistent HPA axis changes, which during protracted withdrawal is characterized by a long-lasting desensitization of the HPA axis responses to subsequent acute ethanol (Hansson et al., 2008; Lee and Rivier, 1997). However, the cellular mechanisms underlying the HPA axis allostatic response to stress in alcohol dependence remain unclear. The aim of this study was to examine the cellular mechanisms by which chronic intermittent ethanol (CIE) treatment, using oral administration, disrupts glutamatergic neurotransmission and synaptic plasticity of PNCs, and relate them to the stress-induced hormonal responses and coping behaviors of rats during protracted withdrawal.

2. MATERIALS AND METHODS

2.1 Animals

All experiments were performed in accordance with the guidance of the National Institutes of Health on animal care and use and the University of California, Los Angeles, Animal Research Committee. Male Sprague Dawley rats (200–300g and ~2 months old) were pair-housed under a 12-hr 6AM/6PM light/dark cycle and had *ad libitum* access to food and water.

Ethanol (Decon Laboratories, King of Prussia, PA) was administered by oral intubation using a chronic intermittent ethanol protocol, referred to as CIE, as it has been previously

described (Cagetti et al., 2003; Kokka et al., 1993; Liang et al., 2007; Liang et al., 2006). Briefly, CIE exposed rats received 5 g/kg of body weight of ethanol as a 25% (w/v) ethanol solution in drinking water once every other day for the first 5 doses, and they received 6 g/kg of body weight of ethanol as a 30% (w/v) ethanol solution once every day for the following 30 doses, for a total of 35 doses (Fig. 1A). Oral administration of ethanol was preferred over vapor administration or intraperitoneal injections as the former is able to mimic alcohol ingestion in humans. With this regimen, blood ethanol concentration (BEC) reached ~270 mg/dl (~60mM) one hour after oral administration of ethanol 5g/kg, and was equivalent to the BEC obtained one hour after intraperitoneal injection of ethanol 3g/kg (Liang et al., 2007). Moreover, rats experience multiple cycles of ethanol intoxication and withdrawal phases leading to a kindling-like state with persistent decrease in pentylenetetrazol seizure threshold (Kokka et al., 1993), and modulation of $GABA_A$R-mediated inhibition and AMPAR-mediated excitation in different brain regions (Liang et al., 2014; Liang et al., 2007; Liang et al., 2006; Marty and Spigelman, 2012). The chronic intermittent vehicle (CIV) groups, corresponding to each CIE treatment, received drinking water (20 ml/kg of body weight) instead of ethanol. After the CIE/CIV treatments, rats experienced 40–60 days of protracted withdrawal in their home cages reaching a body weight of 400–500g (~3.5 to 4 months old). A separate group of naïve control rats (400–500g and ~3.5 to 4 months old) were also used in select electrophysiological studies. Stressed rats were confined in a Plexiglas restrainer (Braintree Scientific, Braintree, MA) for 30 min beginning at 10AM. Data evaluating ACTH, CORT, and self-grooming behavior were collected from the same rats.

2.2 Electrophysiology

Following 40–60 days of protracted withdrawal, rats (400–500g and ~3.5 to 4 months old) were deeply anesthetized with isoflurane (Patterson Veterinary, MA, USA), decapitated, and the brain quickly removed. For stress experiments, rats were anesthetized immediately after stress. Coronal brain slices (400 μm) containing the hypothalamus were obtained with a vibrating slicer (VT1200S, Leica, Buffalo Grove, IL). Before recording, slices were incubated for ≥1hr at room temperature in artificial cerebrospinal fluid (ACSF) containing (in mM): 125 NaCl, 2.5 KCl, 1.25 NaH_2PO_4, 2 $CaCl_2$, 2 $MgCl_2$, 26 $NaHCO_3$, 10 glucose, saturated with 95% O_2 and 5% CO_2.

Whole-cell patch clamp recordings were obtained from PNCs, as defined by their electrophysiological characteristics (Hoffman et al., 1991; Hoyda et al., 2009; Luther et al., 2002; Melnick et al., 2007; Sterley et al., 2018; Stern, 2001; Wamsteeker Cusulin et al., 2013b), during perfusion with ACSF at 34±0.5°C. PNCs were recorded from the dorsal zone of the medial parvocellular part of the PVN, where high density of CRF-expressing PNCs has been described in rats (Simmons and Swanson, 2009) (Fig. 1B). Only the data from cells expressing the PNC electrophysiological characteristics were included. We did not directly examine the neuroendocrine phenotype. However, based on the studies mentioned above, PNCs recorded were most likely neuroendocrine neurons expressing CRF. Patch clamp recording pipettes (TW150F-3, WPI, FL, USA) with 4–5 MΩ resistance were filled with a solution containing (in mM): 130 K-gluconate, 5 NaCl, 1.1 EGTA, 2 MgATP, 0.2 NaGTP, and 10 HEPES, pH adjusted to 7.3 with KOH. Input resistance was calculated in current-

clamp by measuring the changes in the resting membrane potential (RMP) in response to a hyperpolarizing step (−50 pA). Action potential (AP) threshold was measured at the beginning of the sharp upward rise of the depolarizing phase of the first AP elicited by a depolarizing step. Input-output curve was obtained by calculating the number of APs elicited in response to depolarizing currents steps (10 pA increments).

Excitatory postsynaptic currents (EPSCs) were evoked using a concentric bipolar stimulating electrode (MCE-100, Rhodes Medical Instruments, CA, USA) placed in the periventricular aspect (Marty et al., 2011). The stimulus intensity was chosen to elicit ~50% maximum amplitude of the first evoked current. Paired-pulse ratios (PPRs) were obtained by applying a pair of synaptic stimuli of equal intensity applied at a interstimulus interval of 25 ms at a rate of 0.2 Hz as previously described (Kuzmiski et al., 2010; Marty et al., 2011). High frequency afferent stimulation (HFS) used 100 Hz for 1 s, repeated four times with a 5-second interval (Kuzmiski et al., 2010). Access resistance (<30 MΩ) was continuously monitored and recordings were accepted for analysis if changes were <15%. AMPAR-mediated EPSCs were isolated by holding the postsynaptic neuron at −60 mV to block voltage-dependent postsynaptic NMDARs and including the $GABA_A$R antagonist, picrotoxin (50 μM; Tocris Bioscience, MN, USA) in ACSF. In some experiments, NMDAR antagonist MK801 (1 mM; Abcam, MA, USA) was included in the internal solution.

To evaluate AMPAR:NMDAR ratio, AMPAR+NMDAR-mediated spontaneous EPSCs (sEPSCs) were recorded at +40 mV using a pipette solution containing (in mM): 120 CsCl, 10 NaCl, 1.1 EGTA, 0.1 $CaCl_2$, 4 K_2ATP and 0.3 Na_2GTP, 2.5 QX-314, 10 HEPES, pH adjusted to 7.3 with CsOH. After establishment of a 10-min stable baseline, NMDAR antagonist APV (40 μM; Abcam) was applied to isolate the AMPAR-mediated sEPSCs. The amplitude of NMDAR-mediated sEPSCs was calculated by subtracting the averaged isolated AMPAR-mediated sEPSCs from the averaged AMPAR+NMDAR-mediated sEPSCs. AMPAR:NMDAR ratio was the result of the averaged isolated AMPAR-mediated sEPSCs amplitude divided by the calculated NMDAR-mediated sEPSC amplitude for each PNC.

NMDAR-mediated EPSCs were recorded at +40 mV using a pipette solution containing (in mM): 120 CsCl, 10 NaCl, 1.1 EGTA, 0.1 $CaCl_2$, 4 K_2ATP and 0.3 Na_2GTP, 2.5 QX-314, 10 HEPES, pH adjusted to 7.3 with CsOH. For isolation of NMDAR-mediated EPSCs, 6-cyano-7-nitroquinoxaline-2,3-dione (CNQX, 10 μM; Tocris Bioscience) and picrotoxin (50 μM; Tocris Bioscience) were added to the bath to block AMPAR-mediated $GABA_A$R-mediated synaptic currents respectively. In addition, *N*-(2,6-dimethylphenylcarbamoylmethyl) triethyl-ammonium chloride (QX-314, 2.5 mM; Tocris Bioscience) was included in the patch pipette solution to block voltage-gated sodium channels. After establishment of a 10-min stable baseline, ifenprodil (5 μM; Tocris Bioscience) or CRF (1 μM; human/rat, purity ≥99%, Cat#H-2435, Bachem Americas, CA, USA) was bath applied for 6–10 min. In some experiments, ethanol was bath applied at a concentration of 100 mM. This high concentration of ethanol was chosen to induce maximal pharmacological effects as we showed previously (Liang et al., 2007; Liang et al., 2006).

In some experiments, okadaic acid (OA; Alfa Aesar, MA, USA), a blocker of protein phosphatase PP1/PP2A, was dissolved in distilled water (1mM stock) and included in the

patch pipette solution at a concentration of 1 μM, as described previously (Wang et al., 1994; Westphal et al., 1999). In similar experiments, TC-2153 (Sigma-Aldrich, MO, USA), a blocker of striatal-enriched tyrosine protein phosphatase, was dissolved in dimethyl sulfoxide (1 mM stock) and included in the patch pipette solution at a concentration of 1 μM, as described previously (Siemsen et al., 2018; Tian et al., 2016). In these experiments, basal NMDAR-eEPSCs were recorded in the continuous presence of OA or TC-2153. After establishment of a 10-min stable baseline, CRF (1 μM) or ethanol (100 mM) was bath applied for 7–10 min. The effects of CRF or ethanol on NMDARs was examined by comparing the eEPSC amplitude during baseline (2 min prior bath application of CRF or ethanol) and during bath application of CRF or ethanol (last 2 min of application).

Antalarmin, a CRFR1 antagonist, was dissolved in dimethyl sulfoxide to a 1 mM stock solution and was bath applied at a final concentration of 1 μM, according to previous studies (Lemos et al., 2011; Roberto et al., 2010). After establishment of a 10-min stable baseline, antalarmin was bath applied for at least 10 min before co-application of ethanol for 7–8 min. Antalarmin remained for an additional 10–15 min before washout with ACSF. The effects of antalarmin and antalarmin+ethanol on NMDARs was examined by comparing the eEPSC amplitude during baseline (2 min prior to antalarmin), antalarmin (last 2 min of application) and antalarmin+ethanol (last 2 min of application).

Occlusion experiments were performed to assess whether the inhibitory effects of CRF and ethanol on NMDARs were mediated by similar intracellular mechanisms. In these occlusion experiments, ethanol was first bath applied for at least 7 min before co-application of CRF for an additional 7–8 min. Similar occlusion experiments were performed by applying CRF first for at least 7 min before co-application of ethanol for an additional 7–8 min.

Electrophysiological signals were amplified using the Multiclamp 700B amplifier, low-pass filtered at 1 kHz and digitized at 10 kHz with the Digidata 1440A (Molecular Devices, San Jose, CA). Data were acquired using pCLAMP10, low-pass filtered offline at 1kHz and analyzed using Clampfit (Molecular Devices) and MiniAnalysis (Synaptosoft, Decatur, GA) software. AMPAR- and NMDAR-mediated sEPSCs were detected using a threshold equivalent to 2.5 standard deviations from baseline noise. The mean amplitude of spontaneous EPSCs (sEPSCs) was determined by averaging >100 consecutive events. The mean frequency of sEPSCs was determined as the number of events per second during a 60–300 sec period. AMPAR- and NMDAR-mediated eEPSC amplitude was calculated from the baseline current before stimulation to the peak synaptic current. The magnitude of STP was calculated as the average amplitude of 12 eEPSCs immediately following HFS (0–1 min post-HFS) and was expressed as % of baseline.

2.3 Real-time quantitative polymerase chain reaction

TaqMan Gene Expression Master Mix (5 μl, Applied Biosystems, Foster City, CA) mixed with cDNA (4.5μl) and gene-specific primer was used in each qPCR reaction. Reactions for each gene of interest (*Crf*: Rn01462137_m1; *Crhr1*: Rn00578611_m1; *Crhr2*: Rn00575617_m1; *Crf-bp*: Rn00594854_m1; *Nr3c1*: Rn00561369_m1; *Nr3c2*: Rn00565562_m1; *Gapdh*: Rn99999916_s1; Applied Biosystems) were performed in triplicate. RT-qPCR reactions were performed using an ABI7900HT Fast Real-Time PCR

system and the FAM dye. The threshold cycle (C_T) was determined using Sequence Detection System software (Applied Biosystems). Gene expression was normalized to the endogenous control (*Gapdh*) obtaining 2^{-ddC_T}. Statistical differences were evaluated on 2^{-dC_T} (Schmittgen and Livak, 2008).

2.4 Enzyme immunoassay (EIA) determination of ACTH and CORT plasma levels

Tail vein blood was collected into heparinized tubes (Microvette CB300, Starstedt, Germany) pre-stress (0 min) and post-stress (30, 75, and 120 min). Tail vein bleeding technique was chosen based on previous studies measuring plasma levels of stress hormones following acute and repeated stress (Belda et al., 2008; Dal-Zotto et al., 2003; Franco et al., 2016; Gagliano et al., 2008; García et al., 2000; Rabasa et al., 2011; Vahl et al., 2005). A volume of 150–200 μl of blood was collected from the tail vein at each time point. Blood samples were centrifuged at 2,000*g* for 10 min at room temperature. Plasma levels of ACTH (FEK-001–21, Phoenix Pharmaceuticals, Burlingame, CA) and CORT (#500655, Cayman Chemical, Ann Harbor, MI) were assessed using EIA kits as per manufacturer's instructions.

2.5 Self-grooming behavior analysis

After 30 min of acclimatization in the testing room, rats were placed in a new empty cage, similar to the home cage but without bedding, (~10:30 AM) to record baseline self-grooming behavior for 45 min. The video recording was repeated at 7, 10, and 13 days after baseline to measure immediate post-stress self-grooming behavior. Video recordings of the grooming were analyzed off-line by investigators blind to the rats' treatments, as described previously (Kalueff et al., 2007; Kalueff and Tuohimaa, 2005). Total grooming duration, number of grooming episodes (separated by more than 5 seconds of not grooming), and number of rearings, defined as the upward extension of at least half of the rat's body, were analyzed. To overcome the individual differences in time spent exploring, we calculated the fractional time grooming by normalizing the time spent grooming to the time spend exploring for each individual rat, as shown in a previous study (Füzesi et al., 2016). The fractional time grooming was defined as the relative time spent grooming during the rat's active period, allowing a more accurate estimation of the time spent self-grooming. One CIE rat was identified as a statistical outlier (Motulsky and Brown, 2006) and was excluded from the final analysis.

2.6 Statistical Analyses

Data were expressed as mean ± SEM. In all figures, n and N represent the number of PNCs and rats, respectively. Each recorded PNC was treated as individual. PNCs were recorded from at least 3 rats per group. For multiple comparisons, statistical analyses were performed using one- or two-way ANOVA or repeated measures (RM) ANOVA followed by the appropriate post-hoc test. For two group comparisons paired or unpaired Student's *t*-test, nonparametric Mann-Whitney test, or Wilcoxon paired test were used as appropriate, in Prism 7 (GraphPad, San Diego, CA). The effects of various drugs were statistically evaluated using the average amplitude of EPSCs during baseline vs. drug application. Alpha cutoff of 0.05 was used.

3. RESULTS

3.1 CIE exposure induces persistent changes in PNC membrane properties

Analyses of intrinsic membrane properties of PNCs showed that the input resistance was unaffected by stress and CIE treatment (CIV/non-restraint: n=20/N=12; CIE/non-restraint: n=17/N=11; CIV/restraint: n=7/N=5; CIE/restraint: n=13/N=10; two-way ANOVA, $p>0.05$; Fig. 1C). There was a main effect of stress, but not treatment, on the RMP leading to a depolarization of the RMP of PNCs (two-way ANOVA, stress: $F(1,56)=11.51$, $p=0.001$; Fig. 1D). However, post hoc analyses (Sidak's post hoc) showed that stress significantly depolarized PNCs only from CIV rats ($p=0.01$), but not CIE rats ($p=0.14$). There was a main effect of treatment, but not stress, on the AP threshold between CIV and CIE rats (two-way ANOVA, treatment: $F(1,54)=9.5$, $p=0.003$; Fig. 1E). Moreover, the input-output curve was significantly altered by CIE treatment as shown by blunted stress-induced increases in PNC excitability from CIE rats (CIV/non-restraint: n=12/N=9; CIE/non-restraint: n=15/N=9; CIV/restraint: n=7/N=5; CIE/restraint: n=12/N=9; two-way ANOVA, steps: $F(6,249)=54.6$, $p<0.001$, treatment/stress: $F(3,249)=6.7$, $p<0.001$; Tukey's post hoc, CIV/non-restraint vs. CIV/restraint, $p=0.005$; CIV/restraint vs CIE/non-restraint, $p=0.002$; Fig. 1F). These data suggest that CIE exposure increases intrinsic excitability of PNCs, but blunts stress-induced increases in their excitability.

3.2 CIE dysregulates evoked glutamate release

In the presence of picrotoxin (50 μM), AMPAR-sEPSC amplitude did not differ in PNCs from CIV and CIE rats (CIV: n=23/N=15; CIE: n=22/N=17; unpaired t-test, $t(43)=1.59$, $p=0.12$; Fig. 2A–C). AMPAR-sEPSC frequency was also not significantly affected by CIE exposure (unpaired t-test, $t(43)=1.39$, $p=0.17$; Fig. 2A–C). AMPAR-sEPSC rise-time, decay-time and area were unaffected by CIE exposure (not shown). However, the paired-pulse ratio (PPR) of AMPAR-eEPSCs was significantly increased, changing from paired-pulse depression to facilitation in PNCs from CIE rats (CIV: n=10/N=9; CIE: n=14/N=12; unpaired t-test, $t(22)=2.86$, $p=0.009$; Fig. 2D, E). Also, the AMPAR:NMDAR ratio of sEPSCs was significantly decreased in PNCs from CIE compared to CIV rats (CIV: n=10/N=8; CIE: n=9/N=8; unpaired t-test, $t(17)=2.37$, $p=0.029$; Fig. 2F, G). Given that AMPAR-sEPSCs were not affected by CIE exposure, the decreased AMPAR:NMDAR ratio is likely due to increases in NMDAR-mediated currents. These data suggest that CIE exposure produces a long-lasting decrease in presynaptic glutamate release and increases postsynaptic NMDAR function without affecting AMPARs in PNCs.

3.3 CIE increases postsynaptic NMDAR function and decreases ethanol block of NMDARs

As anticipated, CIE exposure significantly increased pharmacologically isolated NMDAR-sEPSC amplitude, but not frequency, compared to CIV rats (Amplitude: CIV: n=28/N=23; CIE: n=26/N=22; unpaired t-test, $t(52)=2.37$, $p=0.0215$; Frequency: CIV: n=23/N=23; CIE: n=22/N=22; unpaired t-test, $t(43)=0.12$, $p=0.9$; Fig. 2H–J). Rise-time and decay-time of NMDAR-mediated currents were analyzed, and no significant differences was observed (data not shown). Furthermore, bath application of GluN2B-containing NMDAR antagonist, ifenprodil (5 μM), significantly decreased NMDAR-sEPSC amplitude in CIE, but not in CIV

rats (CIV: n=8/N=7; Wilcoxon paired test, p=0.11; CIE: n=9/N=8, Wilcoxon paired test, p=0.004; % inhibition CIV vs. CIE, Mann-Whitney test, p=0.036; Fig. 2K, L). This suggests that increased NMDAR function in PNCs of CIE rats is likely mediated by increases in GluN2B-containing NMDARs. We also investigated the effect of ethanol NMDAR-sEPSCs. We found that ethanol-induced decreases in NMDAR-mediated sEPSC amplitude was similar in naïve (paired t-test, p=0.03, n=5/N=4, data not shown) and CIV rats (paired t-test, p=0.007, n=6/N=5; Fig. 2M, N; naïve vs. CIV, unpaired t-test, t(9)=1.02, p=0.33; data not shown). These data suggest that ethanol effects are not altered by vehicle treatment. Furthermore, two-way RMANOVA showed a main effect of ethanol ($F(1,14)=27.57$, $p<0.001$), treatment ($F(1,14)=10.33$, $p=0.006$), and interaction ethanol × treatment ($F(1,14)=10.33$, $p=0.006$). Sidak's post hoc showed that ethanol significantly decreased NMDAR-sEPSC amplitude in CIV, but not in CIE rats (baseline vs. ethanol, CIV: n=6/N=5, $p<0.001$; CIE: n=6/N=5, p=0.39; CIV vs. CIE, $p<0.001$; Fig. 2M, N). This suggests that CIE leads to increased postsynaptic NMDAR function and tolerance of NMDARs to acute ethanol effects.

3.4 CRF-induced depression of NMDAR function is mediated by phosphatase activation

We showed previously that CRF activation of CRFR1 decreases NMDAR function in PNCs (Kuzmiski et al., 2010). As expected, bath application of CRF (1μM, human/rat, purity ≥99%) in the presence of CNQX (10 μM) and picrotoxin (50 μM) decreased NMDAR-eEPSC amplitude in naïve (n=4/N=4, paired t-test, $t(3)=4.25$, p=0.024) and CIV rats (n=8/N=8, paired t-test, $t(7)=4.19$, p=0.004) (Fig. 3A–C). Since no differences were found in CRF-induced decreases in NMDAR-eEPSC amplitude in PNCs from naïve and CIV rats (naïve: 75.6 ± 5 % of baseline, n=4/N=4; CIV: 76.5 ± 5.8 %, n=8/N=8; unpaired t-test, $t(10)=0.1$, p=0.92), data from both groups were combined to compare with the effects of CRF in presence of phosphatase inhibitors (Fig. 3C). Numerous studies have shown that the phosphorylation state of NMDARs is critical in their functional regulation (Morishita et al., 2005; Nijholt et al., 2000; Sheng et al., 2008; Wang et al., 1994; Wang and Salter, 1994). For example, striatal-enriched tyrosine protein phosphatase (STEP) and its interaction with the tyrosine kinase *Fyn* is critical in modulating NMDAR function, as shown by its involvement in ethanol-induced NMDAR inhibition (Miyakawa et al., 1997; Wu et al., 2010). Thus, to further understand the intracellular mechanisms involved in CRF-induced NMDAR depression, an inhibitor of phosphatases PP1 and PP2A, okadaic acid (OA, 1 μM), or a selective STEP blocker, TC-2153 (1 μM), were added to the patch pipette during recordings of PNCs from naïve control rats. In the presence of OA, CRF did not reduce NMDAR-eEPSCs (CRF+OA: n=6/N=4, paired t-test, $t(5)=0.28$, p=0.79; Fig. 3A–C). However, inhibition of NMDAR-eEPSCs by CRF was still observed in presence of TC-2153 (CRF +TC-2153: n=6/N=4, Wilcoxon paired t-test, p=0.031) (Fig. 3A–C). Together, our data showed blunted CRF effects on NMDAR-eEPSCs in presence of OA only (one-way ANOVA ($F(2, 21)=8.21$, p=0.002; Tukey's post-hoc, CRF vs. CRF+OA, p=0.002; CRF vs. CRF+TC-2153, p=0.97; CRF+OA vs. CRF+TC-2153, p=0.01). These data suggest that activation of phosphatases PP1 and/or PP2A by CRF is responsible for the decrease in NMDAR currents in PNCs.

3.5 Ethanol block of NMDARs involves CRFR1 activation

Acute ethanol application inhibits NMDAR function (Lovinger et al., 1989, 1990). Consistently, we found that ethanol (100 mM) reduced NMDAR eEPSC amplitude (n=8/N=7, paired t-test, t(7)=4.89, p=0.0018 vs. baseline; Fig. 3E). Previous studies showed that EtOH-induced changes in synaptic transmission in some brain regions are mediated via CRFR1 activation (Lemos et al., 2011; Nie et al., 2004; Roberto et al., 2010; Silberman et al., 2015). To investigate whether ethanol's inhibition of NMDARs in the PVN is mediated by a CRFR1-dependent mechanism, we bath applied the CRFR1 antagonist, antalarmin (1 μM), prior to application of ethanol. One-way RMANOVA showed no significant effects between baseline, antalarmin and antalarmin+ethanol (n=8/N=7, F(7,14)=0.45, p=0.6; Fig. 3D). The lack of effect of antalarmin alone suggests that NMDAR function is not affected by endogenous CRF. Moreover, the blockade of ethanol effects by antalarmin suggests that ethanol-induced inhibition of NMDARs is dependent on CRFR1 activation. We also found that inhibition of PP1/PP2A prevented ethanol inhibition of NMDAR-eEPSCs (n=5/N=4, paired t-test, t(4)=0.05, p=0.96). Altogether, our data suggest that ethanol-induced inhibition of NMDARs in PNCs depends on CRFR1 and PP1/PP2A activation (one-way ANOVA, F(2,18)=11.76, p<0.001; Tukey's post-hoc, EtOH vs. Antal.+EtOH, p=0.002; EtOH vs. EtOH+OA, p=0.002; Fig. 3E). In occlusion experiments where ethanol was bath applied first followed by CRF co-application, co-application of EtOH+CRF did not further inhibit NMDAR-eEPSCs compared to ethanol alone (n=6/N=5; one-way RMANOVA, treatment: F(5, 10)=30.04, p<0.001; Tukey's post-hoc, baseline vs. EtOH, p<0.001; baseline vs. EtOH +CRF, p=0.008; EtOH vs. EtOH+CRF, p=0.79; Fig. 3E, F). In separate experiments, where CRF was applied first followed by EtOH, a similar occlusion was observed (n=3/N=3, CRF vs. CRF+EtOH, paired t-test, t(2)=2.4, p=0.14; data not shown). Altogether, these data suggest that ethanol inhibition of NMDARs involves a CRFR1-mediated activation of phosphatase(s) PP1 and/or PP2A.

3.6 CIE exposure increases the hypothalamic expression of CRF mRNA

We sought to investigate long-term consequences of CIE exposure on the regulation of stress-related hormones by examining expression of several HPA axis-related genes within the hypothalamus. Compared to CIV rats, mRNA expression levels of only the *Crf* gene were significantly increased in CIE rats (N=4; *Crf*, unpaired t-test, t(6)=5.4, p=0.0017; *Crhr1*, unpaired t-test, t(6)=1.6, p=0.16; *Crhr2*, unpaired t-test, t(6)=0.4, p=0.68; *Crf-bp*, unpaired t-test, t(6)=0.83, p=0.44; *Nr3c1*, unpaired t-test, t(6)=1.0, p=0.34; *Nr3c2*, unpaired t-test, t(6)=0.03, p=0.97; Fig. 4A). These data suggest that CIE increases CRF mRNA expression which may lead to changes in CRF-mediated signaling within the hypothalamus.

3.7 CIE exposure disrupts CRF-induced depression of NMDAR function and acute stress-induced synaptic plasticity

Next, we investigated whether CIE-induced changes in NMDAR function and CRF expression affect CRF-induced inhibition of NMDARs in PNCs. Similar to ethanol, the inhibitory effects of CRF on NMDAR-eEPSCs were impaired in CIE compared to CIV rats (n=8/N=8, CIV: paired t-test, t(7)=4.19, p=0.0041 vs. baseline; n=8/N=7, CIE: paired t-test, t(7)=0.99, p=0.35 vs. baseline; CIV vs. CIE, unpaired t-test, t(14)=3.73, p=0.022; Fig. 4B,

C). CRF-induced depression of NMDAR function is critical for induction of HFS-induced short-term potentiation (STP) of AMPAR-eEPSCs in PNCs following acute restraint (Kuzmiski et al., 2010). To address the consequences of the loss of CRF action, we investigated the effect of CIE on stress-induced synaptic plasticity. As expected, HFS-induced STP, associated with a decrease in PPR, was evoked in PNCs of CIV/restraint rats (n=5/N=5; eEPSC amplitude post-HFS: paired t-test, t(4)=3.72, p=0.02; PPR post-HFS: paired t-test, t(4)=2.84, p=0.04; Fig. 4D, G). However, HFS-induced STP could not be evoked in CIE/restraint rats (n=6/N=5; eEPSC amplitude post-HFS: paired t-test, t(5)=0.25, p=0.8; PPR post-HFS: paired t-test, t(5)=0.47, p=0.7; Fig. 4E, G) suggesting that protracted withdrawal from CIE exposure induces profound alterations in the regulation of stress-induced glutamatergic synaptic plasticity in PNCs.

To test whether the loss of HFS-induced STP in CIE/restraint rats was due to the loss of CRF-mediated NMDAR inhibition after stress, we used an NMDAR antagonist, MK801 (1 mM), in the patch pipettes to inhibit postsynaptic NMDARs specifically in the recorded PNCs. It has been shown previously that inhibition of postsynaptic NMDARs of the recorded PNC using intracellular MK801 unmasked HFS-induced STP in naïve rats (Kuzmiski et al., 2010), suggesting that decreased postsynaptic NMDAR function is required to unmask STP in PNCs. Consistent with this previous study, we also found that intracellular MK801 unmasked HFS-induced STP in CIV/non-restraint rats (n=6/N=3; CIV +iMK801, eEPSC amplitude post-HFS: paired test, t(5)=3.35, p=0.02; PPR post-HFS: paired t-test, t(5)=2.9, p=0.03; grey hatched bar, Fig. 4G), suggesting that PNCs from CIV rats are similar to naïve rats. Furthermore, postsynaptic NMDAR inhibition restored HFS-induced STP in CIE/restraint rats (n=8/N=7; eEPSC amplitude post-HFS: paired t-test, t(7)=5.94, p=0.0006; PPR post-HFS: paired t-test, t(7)=5.66, p=0.0008; one-way ANOVA, F(3,21)=7.17, p=0.002; Dunnett's post-hoc, CIE/restraint vs.: CIV/restraint, p<0.001; CIV/MK801, p=0.01; CIE/restraint+MK801, p=0.007; Fig. 4F, G). Thus, the loss of the CRF-mediated inhibition of NMDAR function via CRFR1 may be responsible for the loss of stress-induced STP in CIE rats.

3.8 CIE alters HPA axis hormonal responses to repeated restraint stress

Plasticity of synapses onto PNCs appears to be an essential mechanism by which the HPA axis adapts its responses to stressors (Sarkar et al., 2011; Wamsteeker et al., 2010). To investigate the physiological consequences of CIE-induced impairment of stress-induced plasticity at glutamatergic synapses onto PNCs, we measured plasma ACTH and CORT levels in response to repeated stress. Rats were subjected to three restraint stresses administered at 72-hour intervals. In CIV rats, similar significant increases in ACTH and CORT plasma levels were found in response to stress 1 and stress 3 at t=30 min (ACTH: N=5, two-way RMANOVA, Stress: F(1,4)=0.15, p=0.72; Time: F(2,8)=22.4, p=0.0005; Dunnett's post-hoc, t=0 vs. t=30, stress 1: p=0.014, stress 3: p=0.044; Fig. 5A; CORT: N=8, two-way RMANOVA, Stress: F(1,7)=0.1, p=0.75; Time: F(3,21)=42.4, p=0.001; Dunnett's post-hoc, t=0 vs. t=30, stress 1: p<0.001, stress 3: p<0.0001; Fig. 5D). The integrated response (area under the curve, AUC) of ACTH and CORT following stress 1 and 3 were similar in CIV rats (ACTH AUC: N=5, paired t-test, p=0.99; Fig. 5A insert; CORT AUC: N=8, paired t-test, p=0.93; Fig. 5D insert). In CIE rats, ACTH and CORT plasma levels were

significantly increased in response to stress 1 at t=30 min. However, both ACTH and CORT responses were significantly reduced following stress 3. Indeed, our data showed significant decreases in the AUC of ACTH and CORT following stress 3 in CIE rats (ACTH AUC: paired t-test, t(5)=3.46, p=0.018; Fig. 5B insert; CORT AUC: N=8, paired t-test, t(7)=2.54, p=0.039; Fig. 5E insert). The blunted ACTH response to stress 3 in CIE rats was associated with a main effect of time and stress, without interaction (ACTH: N=6, two-way RMANOVA, Time: F(2,10)=4.8, p=0.034; Stress: F(1,5)=12, p=0.018; Dunnett's post-hoc, t=0 vs. t=30, stress 1: p=0.002, stress 3: p=0.16; Sidak's post-hoc, Stress 1 vs. Stress 3, t=30: p=0.007; Fig. 5B). Although the magnitude of the CORT response depends on ACTH release, CORT plasma levels at t=30 min post-stress 3 increased in CIE rats similar to CIV rats. However, analysis of the CORT response revealed a main effect of time and stress, without interaction, indicating a faster recovery to baseline (CORT: N=8, two-way RMANOVA, Time: F(3,21)=62.3, p=0.0001; Stress: F(1,7)=7.2, p=0.032; Dunnett's post-hoc, t=0 vs. t=30, stress 1: p<0.001, stress 3: p<0.001; t=0 vs. t=120, stress 1: p=0.8, stress 3: p=0.049; Sidak's post-hoc, stress 1 vs. stress 3: p>0.05; Fig. 5E). Consequently, CORT/ACTH ratio was significantly increased in response to stress 3 at t=30min (N=8, paired-test, t(5)=4.14, p=0.009; Fig. 5F) in CIE rats, suggesting enhanced adrenal sensitivity to ACTH. No difference in CORT/ACTH ratio was found in CIV rats between stress 1 and 3 (N=5, paired t-test, t(4)=0.2, p=0.86; Fig. 5C). These data collectively demonstrate that CIE exposure alters HPA axis function during protracted withdrawal, resulting in a dysregulated neuroendocrine response to repeated homotypic stress.

3.9 CIE impairs self-grooming adaptive behavior

PNCs within the PVN are critical for self-grooming behaviors (Füzesi et al., 2016; Kruk et al., 1998; Mönnikes et al., 1992; Van Erp et al., 1991). In rodents, self-grooming behaviors are elicited following a stressful event, as well as local injection of CRF or ACTH within the PVN (Kalueff and Tuohimaa, 2005; Kruk et al., 1998; Mönnikes et al., 1992; Spruijt et al., 1992). Thus, self-grooming has been considered an adaptive stress-coping behavior (Spruijt et al., 1992). To investigate the behavioral consequences of CIE-induced changes in the CRF and glutamatergic systems within the PVN, we examined whether self-grooming behavior was altered in CIE rats. To determine whether the lack of the relative changes in time spent self-grooming was due to relative changes in the global activity of the rat, we calculated for each rat the fractional time self-grooming after exclusion of time spent inactive/sleeping. While basal exploring time was unchanged (unpaired t-test, t(29)=1.42, p=0.17; data not shown), basal fractional time self-grooming was significantly increased in CIE rats (Fig. 1S). Basal rearing count was lower in CIE rats, which could contribute to increased basal grooming in CIE rats (Fig. 1S).

Analysis of normalized fractional grooming time revealed significant effects of stress and treatment consistent with increases in stress-induced fractional grooming in CIV rats and a blunted response to stress in CIE rats (N=8/group; two-way RMANOVA, Stress: F(3,42)=7.1, p<0.001; Treatment: F(1,14)=7.08 p=0.02; Dunnett's post-hoc; CIV baseline: vs. CIV stress 1, p=0.004; vs. CIV stress 2, p=0.007; vs. CIV stress 3, p<0.001; CIE baseline: vs. CIE stress 1, p=0.75; vs. CIE stress 2, p=0.3; vs. CIE stress 3, p=0.36; Sidak's post-hoc, CIV vs. CIE, stress 3: p=0.02; Fig. 5G). Consistent with a blunted response, stress

did not affect the average episode-length in CIE compared to CIV rats (N=8/group; two-way RMANOVA, Stress: $F(3,42)=6.95$, $p=0.0007$; Treatment: $F(1,14)=10.9$, $p=0.005$; Interaction Stress × Treatment: $F(3,42)=4.2$, $p=0.011$; Sidak's post-hoc, CIV baseline: vs. CIV stress 1, $p=0.006$; vs. CIV stress 2, $p<0.001$; vs. CIV stress 3, $p<0.001$; CIE baseline: vs. CIE stress 1, $p=0.65$; vs. CIE stress 2, $p=0.96$; vs. CIE stress 3, $p=0.84$; CIV vs. CIE: stress 2, $p=0.036$; stress 3: $p=0.002$; Fig. 5H). Moreover, stress induced a significant decrease in rearing in CIV, but not in CIE rats (Fig. 1S). Altogether, these data indicate that CIE exposure results in long-lasting blunting of stress-induced increases in self-grooming, which represents an impairment of adaptive behaviors necessary to effectively cope with stress.

4. DISCUSSION

Adaptive changes in HPA axis function, which lead to altered responses to stress, are most likely mediated by alterations in neuronal synaptic plasticity. Here, we demonstrate that CIE exposure results in long-lasting increases in excitability and altered functional properties of PNCs within the PVN, characterized by increased NMDAR-mediated synaptic currents, loss of ethanol- and CRF-induced decreases in NMDAR function, and impairment of stress-induced depolarization and CRF/NMDAR-dependent adaptive synaptic plasticity. These CIE-induced changes are associated, during protracted withdrawal, with allostatic HPA axis hormonal responses to repeated stress and altered stress coping behaviors.

Although the mechanisms are complex and still being investigated, synaptic NMDARs are critical for HPA axis function. Injections of non-competitive NMDAR antagonists have a stimulatory effect on the HPA axis and stress-induced CRF expression in the PVN (Givalois et al., 2000; Jezová et al., 1995; Lee et al., 1994; Pechnick et al., 1989; Zhou et al., 1998), while stress-induced release of CRF inhibits NMDAR function in PNCs via CRFR1 activation, unmasking STP due to increased presynaptic glutamate release (Kuzmiski et al., 2010). These findings indicate that active NMDARs exert an inhibitory tone on PNCs and the HPA axis under basal conditions. Thus, ethanol's ability to activate the HPA axis may be due to its inhibitory effects on NMDARs in PNCs (Lovinger et al., 1989; Rivier et al., 1984), which we now demonstrate is mediated via CRFR1 activation. Consistent with other brain regions (Iorio et al., 1992; Wang et al., 2010), we showed that CIE exposure resulted in long-lasting increases in GluN2B-containing NMDAR function. Although the small reduction in AMPAR-sEPSC frequency was not significant, we found a reduced paired-pulse depression of AMPAR-eEPSCs in CIE rats, which often indicates decreases in evoked presynaptic glutamate release (Debanne et al., 1996; Marty et al., 2011). Thus, increased NMDAR function could be responsible for the reduction in presynaptic glutamate release probability in PNCs from CIE rats (Kuzmiski et al., 2010). Enhanced endocannabinoid-mediated inhibition of presynaptic neurotransmitter release could also mediate the decreased paired pulse depression in CIE rats, as shown in the ventral tegmental area (Harlan et al., 2018). Together, these data suggest that reduced glutamate release may lead to decreases in the synaptic gain and fidelity of information transfer resulting in the loss of stress-induced synaptic plasticity and allostatic neuroendocrine responses observed in CIE rats (Marty et al., 2011).

Neuroadaptations in extra-hypothalamic CRF systems, such as the extended amygdala, demonstrably contribute to the anxiogenic-like behavior and heightened ethanol intake in ethanol-dependent rats (Rimondini et al., 2002; Roberto et al., 2010; Sommer et al., 2008; Valdez et al., 2002; Valdez et al., 2003). In contrast, the mechanisms underlying the dysregulated hypothalamic CRF system, suggested to play a pivotal role in the allostatic state of HPA axis function (Rivier, 2014), have yet to be fully explored. Studies have shown that CRF has a positive autoregulatory feedback on hypothalamic neurons increasing its own expression and CRFR1 expression to maintain HPA axis responsiveness to a subsequent stress (Dallman, 1993; Luo et al., 1994; Parkes et al., 1993). Consistent with previous studies (Roberto et al., 2010; Sommer et al., 2008; Zorrilla et al., 2001), we found that CRF mRNA expression was increased in CIE rats. However, CRFR1 mRNA expression was unchanged. Although CRF mRNA was increased, our findings showed similar basal plasma ACTH and CORT levels in CIE compared to CIV, and a normal and reduced HPA axis hormonal response to acute and repeated stress, respectively. The expression level of mRNA does not always reliably predict the expression level of its corresponding protein (Vogel and Marcotte, 2012), and post-translational disruption limiting the production of CRF protein may be responsible for the lack of increases in CRF release and PVN activity. In addition, our data showed a decrease in CRF sensitivity of NMDARs and CRF-mediated synaptic plasticity in PNCs from CIE rats. The putative increases in PVN CRF release in response to increased CRF mRNA expression may induce compensatory and adaptive changes reducing the protein expression, ligand binding, or functional activity of CRFRs possibly via post-translational mechanisms (Aguilera et al., 2004; Hauger and Aguilera, 1993). Despite the reduction in CRFR1-mediated CRF signaling in the PVN, our findings showed an allostatic HPA axis response to repeated stress with a normal hormonal response to acute stress. Although the CRF system is necessary for the hormonal response to stress, the HPA axis responsiveness has been shown to also be depend on other modulators such as glucocorticoids and vasopressin (AVP). For example, AVP, which is co-released with CRF in the median eminence (Antoni, 1993; Whitnall et al., 1985), can synergize with CRF to amplify ACTH release (Gillies et al., 1982; Hauger and Aguilera, 1993). Indeed, it has been suggested that AVP may play a critical role in maintaining homeostatic HPA axis hormonal response to acute novel (heterotypic) stress in rats adapted to repeated homotypic stress (Hauger and Aguilera, 1993; Ma et al., 1999).

CRF-induced inhibition of NMDARs via CRFR1 is required for stress-induced STP (Kuzmiski et al., 2010). Indeed, a recent study has shown that photoactivation of CRF-containing PNCs unmasked stress-induced STP, while photoinhibition prevented it (Sterley et al., 2018). Here, we found that intracellular blockade of NMDARs to mimic CRF-induced NMDAR inhibition was sufficient to restore stress-induced STP in CIE rats. This suggests that CIE-induced loss of acute stress-induced STP is likely due to increased function and decreased CRF sensitivity of NMDARs. While the mechanisms underlying CRF effects on NMDARs are still unclear, it has been suggested that CRF affects the membrane distribution and/or phosphorylation state of NMDARs (Fu and Neugebauer, 2008; Ji et al., 2013; Ungless et al., 2003). In the hippocampus, CRF-induced depression of NMDARs is mediated by the activation of PLC/inositol-1,4,5-triphosphate receptor and PLC/PKC pathways (Sheng et al., 2008). In PNCs, we are the first to show that CRF-mediated

inhibition of NMDARs involve the activation of serine/threonine phosphatases PP1 and/or PP2A, key modulators of NMDAR function in the hypothalamus and other brain regions (Jouvenceau et al., 2003; Morishita et al., 2005; Nijholt et al., 2000; Wang et al., 1994; Westphal et al., 1999).

Although several studies have investigated the effects of ethanol-induced inhibition of NMDARs, the mechanisms involved remain controversial (Hughes et al., 2013; Ren et al., 2012; Smothers and Woodward, 2016; Wright et al., 1996; Wu et al., 2010; Zhao et al., 2015). Previous studies have shown that ethanol effects on synaptic transmission were dependent on CRFR1 activation in several brain regions (Lemos et al., 2011; Nie et al., 2004; Roberto et al., 2010; Silberman et al., 2015). Here we show that ethanol-induced NMDAR depression in the PVN is also mediated via CRFR1-dependent mechanisms involving PP1/PP2A. Acute ethanol stimulation of the HPA axis was demonstrated to require CRF activity in the hypothalamus (Lee et al., 2004; Ogilvie et al., 1997; Rivest and Rivier, 1994; Rivier et al., 1984), which suggests that acutely, ethanol may induce CRF release from PNCs with the resultant inhibition of NMDARs. This is consistent with the common intracellular pathways involved in CRF and ethanol effects on NMDARs, and the concomitant loss of their inhibitory effects on NMDARs in CIE rats. The reduced CRF and ethanol sensitivity of PNC NMDARs may explain the blunted HPA axis response to acute ethanol in CIE rats (Lee and Rivier, 1997, 2003; Richardson et al., 2008; Rivier and Vale, 1987). Tolerance of NMDARs to acute ethanol effects has been found in several other (Grover et al., 1994; Grover et al., 1998; Kash et al., 2009; Miyakawa et al., 1997; Wu et al., 2010), but not all (Floyd et al., 2003; Roberto et al., 2004b; Sparta et al., 2013), brain regions following chronic ethanol exposure. In addition to dysregulation of intracellular pathways (Simms et al., 2014), several other mechanisms could also account for the loss of CRF-mediated NMDAR inhibition, including changes in the affinity of CRF for its receptors (Ungless et al., 2003) and/or reorganization of NMDAR subunit composition (Smothers and Woodward, 2016; Zhao et al., 2015).

Basal plasma levels of ACTH and CORT measured in this study were found to be higher than normal basal levels published in previous studies (Belda et al., 2008; Dal-Zotto et al., 2003; Franco et al., 2016; Gagliano et al., 2008; García et al., 2000; Rabasa et al., 2011). These higher basal ACTH and CORT levels observed could be due to the tail vein sampling technique used. Although tail vein bleeding has been found to be suitable for measuring plasma stress hormone levels in rats, the procedure needs to be completed rapidly, under 3 minutes, to achieve true basal values and avoid the initiation of the pituitary response to stress (Vahl et al., 2005). This limitation of the technique may account for the higher basal plasma hormone levels, which may not accurately represent the normal basal levels. Although basal plasma levels were higher, tail vein sampling did not alter ACTH and CORT responses to stress compared to catheter blood sampling and accurately reflect the HPA axis response to stress (Vahl et al., 2005). Thus, since the same experimenter used the same procedure across our study, we believe that the differences, or lack of, in plasma levels of ACTH and CORT observed between groups reflect an accurate assessment of the effects of CIE on HPA axis function in response to stress.

The CIE-induced persistent changes in CRF action and synaptic properties of PNCs during protracted withdrawal likely contribute to the dysregulation of the HPA axis, which in humans is associated with alcohol relapse outcomes (Adinoff et al., 2005; Brady et al., 2006; Junghanns et al., 2003; Sinha et al., 2009; Zorrilla et al., 2001). Consistent with previous studies (Rimondini et al., 2002; Zorrilla et al., 2001), we found that during protracted withdrawal from CIE, the ACTH and CORT plasma levels before and after a single restraint stress were similar to those in CIV rats. This could be due to the demonstrated increase in CRF expression and consequently greater CRF release during stress to compensate for a possible desensitization of CRF-induced ACTH release. The apparently normal hormonal output after a single stressor could also be due to the long period of protracted withdrawal (>40 days), as normal CORT levels and HPA axis responses have been found in some studies of abstaining alcoholics, and non-human primates and rodents with more than 4–6 weeks of forced withdrawal, suggesting that HPA axis activity is dynamic and changes during abstinence (Adinoff et al., 1990; Boyd et al., 2010; Coiro et al., 2007; Jimenez et al., 2015; Zorrilla et al., 2001). Also, rodents are studied in highly controlled environments that are impossible to mimic in human studies. Thus, the persistently blunted HPA axis response to stressors observed in human alcoholics could have been in response to a succession of stressors prior to testing.

Acute and chronic stress induce neuroadaptive changes of synaptic transmission of PNCs thereby affecting HPA axis function (Hewitt et al., 2009; Inoue et al., 2013; Kusek et al., 2013; Kuzmiski et al., 2010; Sterley et al., 2018; Wamsteeker Cusulin et al., 2013a; Wamsteeker et al., 2010). Although acute stress unmasks CRF-mediated HFS-induced STP in control rats, its precise role in HPA axis activation is still unknown. However, a recent study has shown that selective disruption of CRFR1 function within the PVN impaired the HPA axis responses to repeated, but not acute, stress (Ramot et al., 2017). Similarly, we found that CIE exposure altered the HPA axis hormonal responses to repeated, but not acute, stress. Taken together, these data suggest that NMDARs and stress-induced STP may be critical to the HPA axis adaptive responses to repeated, but no acute stress (Bains et al., 2015). The lack of CIE effect on the HPA axis response to acute stress could also be due to compensatory mechanisms induced to counterbalance the maladaptive changes. GABAergic transmission was demonstrated to become excitatory following acute stress due to a collapse of the chloride gradient (Hewitt et al., 2009; Sarkar et al., 2011). Since CIE exposure alters GABAergic synaptic transmission in different brain regions (Cagetti et al., 2003; Harlan et al., 2018; Liang et al., 2007; Liang et al., 2006; Lindemeyer et al., 2014; Roberto et al., 2004a), it is possible that $GABA_A$R-mediated excitatory drive is increased following acute stress in CIE rats. Stress also causes several alterations in PNC GABAergic synaptic plasticity, which could affect HPA axis output (Inoue et al., 2013; Wamsteeker Cusulin et al., 2013a; Wamsteeker et al., 2010).

Consistent with previous studies (Kant et al., 1985; Pitman et al., 1988), we show that repeated restraint stress did not change ACTH and CORT responses in control rats. Importantly, we found that the hormonal responses to repeated restraint stress were blunted in CIE rats. After the 3rd stress, peak ACTH response was strongly reduced, and the recovery of CORT levels was enhanced. The increased CORT/ACTH ratio in response to the 3rd stress, suggestive of enhanced adrenal sensitivity to ACTH, is characteristic of the CIE-

induced allostatic load and predictive of stress-induced relapse in alcoholics (Sinha et al., 2011). Together these findings suggest that the loss of CRF-mediated NMDAR blockade and the consequent loss of stress-induced STP in PNCs contribute to the blunted HPA axis hormonal response to repeated homotypic stressors in CIE rats.

In concert with the physiological changes mediated by HPA axis activation, a stressful stimulus triggers specific behavioral responses that improve chances for survival and adaptation in a hostile or new environment (Blanchard et al., 2011; Henson et al., 2012; Sterley et al., 2018). Following a stressful event, rodents exhibit coping behaviors related to vigilance and environmental risk assessment. These include exploration and rearing, as well as self-directed behaviors, such as self-grooming. Post-stress increase in self-grooming is an adaptive process of restoring behavioral homeostasis disturbed by anxiogenic stimuli (Kalueff and Tuohimaa, 2005; Kruk et al., 1998; Spruijt et al., 1992; van Erp et al., 1994). ACTH was the first peptide reported to induce excessive grooming (Ferrari, 1958). Compared to other peptides, intracerebroventricular or intracisternal injections of ACTH induces grooming behavior with characteristics similar to spontaneous grooming with identical cephalo-caudal order within bouts (Gispen and Isaacson, 1981; Sachs, 1988). Moreover, both ACTH and stress were found to produce similar increases in grooming bouts (Aloyo et al., 1983; Dunn et al., 1979; Gispen and Isaacson, 1981; Spruijt et al., 1992). Interestingly, ACTH-induced excessive grooming is not dependent on the release of adrenal glucocorticoids (Gispen et al., 1975; Wiegant et al., 1979). Together, these studies suggest that ACTH plays a critical role in the mechanisms underlying stress-induced increased grooming. Thus, the impaired stress-induced increases in grooming observed in CIE rats could be due to the reduced ACTH response to stress. The inability for CIE rats to increase plasma ACTH levels after stress may result in the lack of activation of neural subtrates necessary to elicit increases in self-grooming behavior.

Intracerebroventricular injections of CRF also mimic stress-induced increases in self-grooming (Dunn et al., 1987). Interestingly, stress-induced self-grooming predicts enhanced motivation to self-administer cocaine (Homberg et al., 2002). Although other brain regions have been shown to modulate self-grooming, recent evidence supports a central role of CRF-expressing PNCs within the PVN in regulating both basal and stress-induced self-grooming. Thus, selective photostimulation of CRF-expressing PNCs was shown to increase self-grooming and decrease rearing behaviors (Füzesi et al., 2016). Consistent with the increased basal excitability of PNCs (cf. Fig. 1E) CIE rats exhibited increased basal fractional time grooming and decreased rearing. This suggests that CIE facilitates self-directed behaviors in detriment of purposeful exploratory behaviors. We also found that CIE rats exhibited blunted stress-induced increases in excitability of PNCs (cf. Fig. 1F) and in self-grooming (cf. Fig. 5G). Interestingly, photoinhibition of CRF-expressing PNCs impairs stress-induced increases in self-grooming (Füzesi et al., 2016). This suggests that loss of stress-induced membrane depolarization and stress-induced STP (cf. Fig. 4) could contribute to the impairment of self-grooming in stressed CIE rats. It will be interesting to determine if restoring stress-induced STP by acute PVN infusion of MK801 could rescue adaptive self-grooming in CIE rats.

Stress-induced STP in PVN CRF neurons was recently shown to be necessary for triggering adaptive behaviors required for investigating and detecting alarm pheromones to communicate information about a stressful event and social transfer of STP in PNCs to conspecific partners not exposed to danger directly (Sterley et al., 2018). It will be interesting to determine if CIE-induced loss of stress-induced STP would also disrupt these specific social behaviors, thereby contributing to reduced social interactions and negative emotions characteristic of AUD (Koob, 2015; Overstreet et al., 2002).

Increased basal stereotyped behaviors associated with dysregulated stress-induced coping behaviors have been linked to psychiatric disorders in which individuals turn their focus towards self-directed behaviors while ignoring the environment cues to alleviate their negative emotions (Gilmer and McKinney, 2003). Thus, the blunting effect of CIE on these adaptive behaviors could be responsible for the allostatic coping behaviors and exaggerated ethanol intake induced by stress in CIE rats (Sommer et al., 2008; Valdez et al., 2003).

5. Conclusions

In this study, we demonstrated persistent alterations of the membrane properties and glutamatergic synaptic plasticity of PVN PNCs and related them to the dysregulated hormonal and behavioral responses of the HPA axis to repetitive stressors in CIE rats. Further investigations of CIE-induced adaptive changes within the PVN neuronal network should extend our understanding of the cellular mechanisms responsible for the persistent allostatic state in AUD.

Supplementary Material

Refer to Web version on PubMed Central for supplementary material.

Acknowledgements

We would like to thank Junwei Li, David H. Terry, Marijo Pempeña, Andrew Liao, and Stephanie Yee for their help in the analysis.

Funding and Disclosure

This work was supported by NIH/NIAAA [grant numbers AA022707 and AA024527]. J.J. Munier was supported by NIH/NIDA [grant number T32DA024635]. The authors declare no competing financial interests.

Abbreviations:

ACTH	adrenocorticotropic hormone
AMPAR	α-amino-3-hydroxy-5-methyl-4-isoxazolepropionic acid
Antal	antalarmin
AUC	area under the curve
AUD	alcohol use disorder
CIE	chronic intermittent ethanol

CIV	chronic intermittent vehicle
CORT	corticosterone
CRF	corticotropin-releasing factor
CRFR1	CRF1 receptor
CRFR2	CRF2 receptor
EIA	enzyme immunoassay
EPSC	excitatory postsynaptic current
EtOH	ethanol
HFS	high frequency stimulation
HPA axis	hypothalamic-pituitary-adrenal axis
NMDAR	N-methyl-D-aspartate receptor
PNC	parvocellular neurosecretory cell
PP1	protein phosphatase 1
PP2A	protein phosphatase 2A
PPR	paired-pulse ratio
PVN	paraventricular nucleus of the hypothalamus
STEP	striatal-enriched tyrosine protein phosphatase
STP	short-term synaptic potentiation

References

Adinoff B, Junghanns K, Kiefer F, Krishnan-Sarin S, 2005 Suppression of the HPA axis stress-response: implications for relapse. Alcohol Clin Exp Res 29, 1351–1355. 10.1097/01.alc.0000176356.97620.84. [PubMed: 16088999]

Adinoff B, Martin PR, Bone GH, Eckardt MJ, Roehrich L, George DT, Moss HB, Eskay R, Linnoila M, Gold PW, 1990 Hypothalamic-pituitary-adrenal axis functioning and cerebrospinal fluid corticotropin releasing hormone and corticotropin levels in alcoholics after recent and long-term abstinence. Arch Gen Psychiatry 47, 325–330. 10.1097/01.alc.0000176356.97620.84. [PubMed: 2157379]

Aguilera G, Nikodemova M, Wynn PC, Catt KJ, 2004 Corticotropin releasing hormone receptors: two decades later. Peptides 25, 319–329. 10.1016/j.peptides.2004.02.002. [PubMed: 15134857]

Aloyo VJ, Spruijt B, Zwiers H, Gispen WH, 1983 Peptide-induced excessive grooming in the rat: the role of opiate receptors. Peptides 4, 833–836. 10.1016/0196-9781(83)90076-1. [PubMed: 6324139]

Antoni FA, 1993 Vasopressinergic control of pituitary adrenocorticotropin secretion comes of age. Front Neuroendocrinol 14, 76–122. 10.1006/frne.1993.1004. [PubMed: 8387436]

Bains JS, Wamsteeker Cusulin JI, Inoue W, 2015 Stress-related synaptic plasticity in the hypothalamus. Nat Rev Neurosci 16, 377–388. 10.1038/nrn3881. [PubMed: 26087679]

Bale TL, Vale WW, 2004 CRF and CRF receptors: role in stress responsivity and other behaviors. Annu Rev Pharmacol Toxicol 44, 525–557. 10.1146/annurev.pharmtox.44.101802.121410. [PubMed: 14744257]

Belda X, Fuentes S, Nadal R, Armario A, 2008 A single exposure to immobilization causes long-lasting pituitary-adrenal and behavioral sensitization to mild stressors. Horm Behav 54, 654–661. 10.1016/j.yhbeh.2008.07.003. [PubMed: 18675818]

Blanchard DC, Griebel G, Pobbe R, Blanchard RJ, 2011 Risk assessment as an evolved threat detection and analysis process. Neurosci Biobehav Rev 35, 991–998. 10.1016/j.neubiorev.2010.10.016. [PubMed: 21056591]

Boyd KN, Kumar S, O'Buckley TK, Morrow AL, 2010 Chronic ethanol exposure produces tolerance to elevations in neuroactive steroids: mechanisms and reversal by exogenous ACTH. J Neurochem 115, 142–152. 10.1111/j.1471-4159.2010.06904.x. [PubMed: 20633208]

Brady KT, Back SE, Waldrop AE, McRae AL, Anton RF, Upadhyaya HP, Saladin ME, Randall PK, 2006 Cold pressor task reactivity: predictors of alcohol use among alcohol-dependent individuals with and without comorbid posttraumatic stress disorder. Alcohol Clin Exp Res 30, 938–946. 10.1111/j.1530-0277.2006.00097.x. [PubMed: 16737451]

Cagetti E, Liang J, Spigelman I, Olsen RW, 2003 Withdrawal from chronic intermittent ethanol treatment changes subunit composition, reduces synaptic function, and decreases behavioral responses to positive allosteric modulators of GABAA receptors. Mol Pharmacol 63, 53–64. 10.1124/mol.63.1.53. [PubMed: 12488536]

Coiro V, Casti A, Jotti GS, Rubino P, Manfredi G, Maffei ML, Melani A, Volta E, Chiodera P, 2007 Adrenocorticotropic hormone/cortisol response to physical exercise in abstinent alcoholic patients. Alcohol Clin Exp Res 31, 901–906. 10.1111/j.1530-0277.2007.00376.x. [PubMed: 17386066]

Dal-Zotto S, Martí O, Armario A, 2003 Glucocorticoids are involved in the long-term effects of a single immobilization stress on the hypothalamic-pituitary-adrenal axis. Psychoneuroendocrinology 28, 992–1009. 10.1016/s0306-4530(02)00120-8. [PubMed: 14529704]

Dallman MF, 1993 Stress update Adaptation of the hypothalamic-pituitary-adrenal axis to chronic stress. Trends Endocrinol Metab 4, 62–69. 10.1016/s1043-2760(05)80017-7. [PubMed: 18407136]

Debanne D, Guérineau NC, Gähwiler BH, Thompson SM, 1996 Paired-pulse facilitation and depression at unitary synapses in rat hippocampus: quantal fluctuation affects subsequent release. J Physiol 491 (Pt 1), 163–176. 10.1113/jphysiol.1996.sp021204. [PubMed: 9011608]

Dunn AJ, Berridge CW, Lai YI, Yachabach TL, 1987 CRF-induced excessive grooming behavior in rats and mice. Peptides 8, 841–844. 10.1016/0196-9781(87)90069-6. [PubMed: 3501576]

Dunn AJ, Green EJ, Isaacson RL, 1979 Intracerebral adrenocorticotropic hormone mediates novelty-induced grooming in the rat. Science 203, 281–283. 10.1126/science.216073. [PubMed: 216073]

Ferrari W, 1958 Behavioural changes in animals after intracisternal injection with adrenocorticotrophic hormone and melanocyte-stimulating hormone. Nature 181, 925–926. 10.1038/181925a0. [PubMed: 13526737]

Floyd DW, Jung KY, McCool BA, 2003 Chronic ethanol ingestion facilitates N-methyl-D-aspartate receptor function and expression in rat lateral/basolateral amygdala neurons. J Pharmacol Exp Ther 307, 1020–1029. 10.1124/jpet.103.057505. [PubMed: 14534353]

Franco AJ, Chen C, Scullen T, Zsombok A, Salahudeen AA, Di S, Herman JP, Tasker JG, 2016 Sensitization of the Hypothalamic-Pituitary-Adrenal Axis in a Male Rat Chronic Stress Model. Endocrinology 157, 2346–2355. 10.1210/en.2015-1641. [PubMed: 27054552]

Fu Y, Neugebauer V, 2008 Differential mechanisms of CRF1 and CRF2 receptor functions in the amygdala in pain-related synaptic facilitation and behavior. J Neurosci 28, 3861–3876. 10.1523/JNEUROSCI.0227-08.2008. [PubMed: 18400885]

Füzesi T, Daviu N, Wamsteeker Cusulin JI, Bonin RP, Bains JS, 2016 Hypothalamic CRH neurons orchestrate complex behaviours after stress. Nat Commun 7, 11937 10.1038/ncomms11937. [PubMed: 27306314]

Gagliano H, Fuentes S, Nadal R, Armario A, 2008 Previous exposure to immobilisation and repeated exposure to a novel environment demonstrate a marked dissociation between behavioral and pituitary-adrenal responses. Behav Brain Res 187, 239–245. 10.1016/j.bbr.2007.09.006. [PubMed: 17945358]

García A, Martí O, Vallès A, Dal-Zotto S, Armario A, 2000 Recovery of the hypothalamic-pituitary-adrenal response to stress. Effect of stress intensity, stress duration and previous stress exposure. Neuroendocrinology 72, 114–125. 10.1159/000054578. [PubMed: 10971146]

Gillies GE, Linton EA, Lowry PJ, 1982 Corticotropin releasing activity of the new CRF is potentiated several times by vasopressin. Nature 299, 355–357. 10.1038/299355a0. [PubMed: 6287293]

Gilmer WS, McKinney WT, 2003 Early experience and depressive disorders: human and non-human primate studies. J Affect Disord 75, 97–113. [PubMed: 12798250]

Gispen WH, Isaacson RL, 1981 ACTH-induced excessive grooming in the rat. Pharmacol Ther 12, 209–246. 10.1016/0163-7258(81)90081-4. [PubMed: 6114501]

Gispen WH, Wiegant VM, Greven HM, de Wied D, 1975 The induction of excessive grooming in the rat by intraventricular application of peptides derived from ACTH: structure-activity studies. Life Sci 17, 645–652. 10.1016/0024-3205(75)90103-4. [PubMed: 171535]

Givalois L, Arancibia S, Tapia-Arancibia L, 2000 Concomitant changes in CRH mRNA levels in rat hippocampus and hypothalamus following immobilization stress. Brain Res Mol Brain Res 75, 166–171. 10.1016/S0169-328X(99)00290-9. [PubMed: 10648901]

Grover CA, Frye GD, Griffith WH, 1994 Acute tolerance to ethanol inhibition of NMDA-mediated EPSPs in the CA1 region of the rat hippocampus. Brain Res 642, 70–76. 10.1016/0006-8993(94)90906-7. [PubMed: 7913393]

Grover CA, Wallace KA, Lindberg SA, Frye GD, 1998 Ethanol inhibition of NMDA currents in acutely dissociated medial septum/diagonal band neurons from ethanol dependent rats. Brain Res 782, 43–52. 10.1016/S0006-8993(97)01001-9. [PubMed: 9519248]

Hansson AC, Rimondini R, Neznanova O, Sommer WH, Heilig M, 2008 Neuroplasticity in brain reward circuitry following a history of ethanol dependence. Eur J Neurosci 27, 1912–1922. 10.1111/j.1460-9568.2008.06159.x. [PubMed: 18412612]

Harlan BA, Becker HC, Woodward JJ, Riegel AC, 2018 Opposing actions of CRF-R1 and CB1 receptors on VTA-GABAergic plasticity following chronic exposure to ethanol. Neuropsychopharmacology 43, 2064–2074. 10.1038/s41386-018-0106-9. [PubMed: 29946104]

Hauger RL, Aguilera G, 1993 Regulation of pituitary corticotropin releasing hormone (CRH) receptors by CRH: interaction with vasopressin. Endocrinology 133, 1708–1714. 10.1210/endo.133.4.8404613. [PubMed: 8404613]

Heilig M, Koob GF, 2007 A key role for corticotropin-releasing factor in alcohol dependence. Trends Neurosci 30, 399–406. 10.1016/j.tins.2007.06.006. [PubMed: 17629579]

Henson SM, Weldon LM, Hayward JL, Greene DJ, Megna LC, Serem MC, 2012 Coping behaviour as an adaptation to stress: post-disturbance preening in colonial seabirds. J Biol Dyn 6, 17–37. 10.1080/17513758.2011.605913 [PubMed: 22873521]

Herman JP, Cullinan WE, Ziegler DR, Tasker JG, 2002 Role of the paraventricular nucleus microenvironment in stress integration. Eur J Neurosci 16, 381–385. 10.1046/j.1460-9568.2002.02133.x. [PubMed: 12193178]

Hewitt SA, Wamsteeker JI, Kurz EU, Bains JS, 2009 Altered chloride homeostasis removes synaptic inhibitory constraint of the stress axis. Nat Neurosci 12, 438–443. 10.1038/nn.2274. [PubMed: 19252497]

Hoffman NW, Tasker JG, Dudek FE, 1991 Immunohistochemical differentiation of electrophysiologically defined neuronal populations in the region of the rat hypothalamic paraventricular nucleus. J Comp Neurol 307, 405–416. 10.1002/cne.903070306. [PubMed: 1856330]

Homberg JR, van den Akker M, Raasø HS, Wardeh G, Binnekade R, Schoffelmeer AN, de Vries TJ, 2002 Enhanced motivation to self-administer cocaine is predicted by self-grooming behaviour and relates to dopamine release in the rat medial prefrontal cortex and amygdala. Eur J Neurosci 15, 1542–1550. 10.1046/j.1460-9568.2002.01976.x. [PubMed: 12028365]

Hoyda TD, Samson WK, Ferguson AV, 2009 Adiponectin depolarizes parvocellular paraventricular nucleus neurons controlling neuroendocrine and autonomic function. Endocrinology 150, 832–840. 10.1210/en.2008-1179. [PubMed: 18948398]

Huang MM, Overstreet DH, Knapp DJ, Angel R, Wills TA, Navarro M, Rivier J, Vale W, Breese GR, 2010 Corticotropin-releasing factor (CRF) sensitization of ethanol withdrawal-induced anxiety-

like behavior is brain site specific and mediated by CRF-1 receptors: relation to stress-induced sensitization. J Pharmacol Exp Ther 332, 298–307. 10.1124/jpet.109.159186. [PubMed: 19843974]

Hughes BA, Smothers CT, Woodward JJ, 2013 Dephosphorylation of GluN2B C-terminal tyrosine residues does not contribute to acute ethanol inhibition of recombinant NMDA receptors. Alcohol 47, 181–186. 10.1016/j.alcohol.2012.12.015. [PubMed: 23357553]

Inoue W, Baimoukhametova DV, Fuzesi T, Cusulin JI, Koblinger K, Whelan PJ, Pittman QJ, Bains JS, 2013 Noradrenaline is a stress-associated metaplastic signal at GABA synapses. Nat Neurosci 16, 605–612. . 10.1038/nn.3373. [PubMed: 23563580]

Iorio KR, Reinlib L, Tabakoff B, Hoffman PL, 1992 Chronic exposure of cerebellar granule cells to ethanol results in increased N-methyl-D-aspartate receptor function. Mol Pharmacol 41, 1142–1148. [PubMed: 1535416]

Jezová D, Tokarev D, Rusnák M, 1995 Endogenous excitatory amino acids are involved in stress-induced adrenocorticotropin and catecholamine release. Neuroendocrinology 62, 326–332. 10.1159/000127021. [PubMed: 8544945]

Ji G, Fu Y, Adwanikar H, Neugebauer V, 2013 Non-pain-related CRF1 activation in the amygdala facilitates synaptic transmission and pain responses. Mol Pain 9, 2 10.1186/1744-8069-9-2. [PubMed: 23410057]

Jimenez VA, Helms CM, Cornea A, Meshul CK, Grant KA, 2015 An ultrastructural analysis of the effects of ethanol self-administration on the hypothalamic paraventricular nucleus in rhesus macaques. Front Cell Neurosci 9, 260 10.3389/fncel.2015.00260. [PubMed: 26236193]

Jouvenceau A, Billard JM, Haditsch U, Mansuy IM, Dutar P, 2003 Different phosphatase-dependent mechanisms mediate long-term depression and depotentiation of long-term potentiation in mouse hippocampal CA1 area. Eur J Neurosci 18, 1279–1285. 10.1046/j.1460-9568.2003.02831.x. [PubMed: 12956726]

Junghanns K, Backhaus J, Tietz U, Lange W, Bernzen J, Wetterling T, Rink L, Driessen M, 2003 Impaired serum cortisol stress response is a predictor of early relapse. Alcohol Alcohol 38, 189–193. 10.1093/alcalc/agg052. [PubMed: 12634269]

Kalueff AV, Aldridge JW, LaPorte JL, Murphy DL, Tuohimaa P, 2007 Analyzing grooming microstructure in neurobehavioral experiments. Nat Protoc 2, 2538–2544. 10.1038/nprot.2007.367. [PubMed: 17947996]

Kalueff AV, Tuohimaa P, 2005 The grooming analysis algorithm discriminates between different levels of anxiety in rats: potential utility for neurobehavioural stress research. J Neurosci Methods 143, 169–177. 10.1016/j.jneumeth.2004.10.001. [PubMed: 15814150]

Kant GJ, Eggleston T, Landman-Roberts L, Kenion CC, Driver GC, Meyerhoff JL, 1985 Habituation to repeated stress is stressor specific. Pharmacol Biochem Behav 22, 631–634. 10.1016/0091-3057(85)90286-2. [PubMed: 2986182]

Kash TL, Baucum AJ 2nd, Conrad KL, Colbran RJ, Winder DG, 2009 Alcohol exposure alters NMDAR function in the bed nucleus of the stria terminalis. Neuropsychopharmacology 34, 2420–2429. 10.1038/npp.2009.69. [PubMed: 19553918]

Kokka N, Sapp DW, Taylor AM, Olsen RW, 1993 The kindling model of alcohol dependence: similar persistent reduction in seizure threshold to pentylenetetrazol in animals receiving chronic ethanol or chronic pentylenetetrazol. Alcohol Clin Exp Res 17, 525–531. 10.1111/j.1530-0277.1993.tb00793.x. [PubMed: 8392817]

Koob GF, 2003 Alcoholism: allostasis and beyond. Alcohol Clin Exp Res 27, 232–243. 10.1097/01.ALC.0000057122.36127.C2. [PubMed: 12605072]

Koob GF, 2008 A role for brain stress systems in addiction. Neuron 59, 11–34. 10.1016/j.neuron.2008.06.012. [PubMed: 18614026]

Koob GF, 2015 The dark side of emotion: the addiction perspective. Eur J Pharmacol 753, 73–87. 10.1016/j.ejphar.2014.11.044. [PubMed: 25583178]

Kruk MR, Westphal KG, Van Erp AM, van Asperen J, Cave BJ, Slater E, de Koning J, Haller J, 1998 The hypothalamus: cross-roads of endocrine and behavioural regulation in grooming and aggression. Neurosci Biobehav Rev 23, 163–177. 10.1016/S0149-7634(98)00018-9. [PubMed: 9884110]

Kusek M, Tokarski K, Hess G, 2013 Repeated restraint stress enhances glutamatergic transmission in the paraventricular nucleus of the rat hypothalamus. J Physiol Pharmacol 64, 565–570. [PubMed: 24304570]

Kuzmiski JB, Marty V, Baimoukhametova DV, Bains JS, 2010 Stress-induced priming of glutamate synapses unmasks associative short-term plasticity. Nat Neurosci 13, 1257–1264. 10.1038/nn.2629. [PubMed: 20818385]

Le Moal M, 2009 Drug abuse: vulnerability and transition to addiction. Pharmacopsychiatry 42 Suppl 1, S42–55. 10.1055/s-0029-1216355. [PubMed: 19434555]

Lee S, Craddock Z, Rivier C, 2011 Brain stem catecholamines circuitry: activation by alcohol and role in the hypothalamic-pituitary-adrenal response to this drug. J Neuroendocrinol 23, 531–541. 10.1111/j.1365-2826.2011.02131.x. [PubMed: 21447066]

Lee S, Rivier C, 1997 An initial, three-day-long treatment with alcohol induces a long-lasting phenomenon of selective tolerance in the activity of the rat hypothalamic-pituitary-adrenal axis. J Neurosci 17, 8856–8866. 10.1523/jneurosci.17-22-08856. [PubMed: 9348353]

Lee S, Rivier C, 2003 Long-term influence of an initial exposure to alcohol on the rat hypothalamic-pituitary axis. Alcohol Clin Exp Res 27, 1463–1470. 10.1097/01.alc.0000086065.06203.dd. [PubMed: 14506408]

Lee S, Rivier C, Torres G, 1994 Induction of c-fos and CRF mRNA by MK-801 in the parvocellular paraventricular nucleus of the rat hypothalamus. Brain Res Mol Brain Res 24, 192–198. 10.1016/0169-328X(94)90132-5. [PubMed: 7968357]

Lee S, Selvage D, Hansen K, Rivier C, 2004 Site of action of acute alcohol administration in stimulating the rat hypothalamic-pituitary-adrenal axis: comparison between the effect of systemic and intracerebroventricular injection of this drug on pituitary and hypothalamic responses. Endocrinology 145, 4470–4479. 10.1210/en.2004-0110. [PubMed: 15205375]

Lemos JC, Zhang G, Walsh T, Kirby LG, Akanwa A, Brooks-Kayal A, Beck SG, 2011 Stress-hyperresponsive WKY rats demonstrate depressed dorsal raphe neuronal excitability and dysregulated CRF-mediated responses. Neuropsychopharmacology 36, 721–734. 10.1038/npp.2010.200. [PubMed: 21160465]

Leslie SN, Nairn AC, 2019 cAMP regulation of protein phosphatases PP1 and PP2A in brain. Biochim Biophys Acta Mol Cell Res 1866, 64–73. 10.1016/j.bbamcr.2018.09.006. [PubMed: 30401536]

Li J, Bian W, Dave V, Ye JH, 2011 Blockade of GABA(A) receptors in the paraventricular nucleus of the hypothalamus attenuates voluntary ethanol intake and activates the hypothalamic-pituitary-adrenocortical axis. Addict Biol 16, 600–614. 10.1111/j.1369-1600.2011.00344.x. [PubMed: 21762292]

Liang J, Marty VN, Mulpuri Y, Olsen RW, Spigelman I, 2014 Selective modulation of GABAergic tonic current by dopamine in the nucleus accumbens of alcohol-dependent rats. J Neurophysiol 112, 51–60. 10.1152/jn.00565.2013. [PubMed: 24717351]

Liang J, Suryanarayanan A, Abriam A, Snyder B, Olsen RW, Spigelman I, 2007 Mechanisms of reversible GABAA receptor plasticity after ethanol intoxication. J Neurosci 27, 12367–12377. 10.1523/jneurosci.2786-07.2007. [PubMed: 17989301]

Liang J, Zhang N, Cagetti E, Houser CR, Olsen RW, Spigelman I, 2006 Chronic intermittent ethanol-induced switch of ethanol actions from extrasynaptic to synaptic hippocampal GABAA receptors. J Neurosci 26, 1749–1758. 10.1523/jneurosci.4702-05.2006. [PubMed: 16467523]

Lindemeyer AK, Liang J, Marty VN, Meyer EM, Suryanarayanan A, Olsen RW, Spigelman I, 2014 Ethanol-induced plasticity of GABAA receptors in the basolateral amygdala. Neurochem Res 39, 1162–1170. 10.1007/s11064-014-1297-z. [PubMed: 24710789]

Lovinger DM, White G, Weight FF, 1989 Ethanol inhibits NMDA-activated ion current in hippocampal neurons. Science 243, 1721–1724. 10.1126/science.2467382. [PubMed: 2467382]

Lovinger DM, White G, Weight FF, 1990 NMDA receptor-mediated synaptic excitation selectively inhibited by ethanol in hippocampal slice from adult rat. J Neurosci 10, 1372–1379. 10.1523/jneurosci.10-04-01372.1990. [PubMed: 2158533]

Luo X, Kiss A, Makara G, Lolait SJ, Aguilera G, 1994 Stress-specific regulation of corticotropin releasing hormone receptor expression in the paraventricular and supraoptic nuclei of the

hypothalamus in the rat. J Neuroendocrinol 6, 689–696. 10.1111/j.1365-2826.1994.tb00636.x. [PubMed: 7894472]

Luther JA, Daftary SS, Boudaba C, Gould GC, Halmos KC, Tasker JG, 2002 Neurosecretory and non-neurosecretory parvocellular neurones of the hypothalamic paraventricular nucleus express distinct electrophysiological properties. J Neuroendocrinol 14, 929–932. 10.1046/j.1365-2826.2002.00867.x. [PubMed: 12472873]

Ma XM, Lightman SL, Aguilera G, 1999 Vasopressin and corticotropin-releasing hormone gene responses to novel stress in rats adapted to repeated restraint. Endocrinology 140, 3623–3632. 10.1210/endo.140.8.6943. [PubMed: 10433220]

Marty V, Kuzmiski JB, Baimoukhametova DV, Bains JS, 2011 Short-term plasticity impacts information transfer at glutamate synapses onto parvocellular neuroendocrine cells in the paraventricular nucleus of the hypothalamus. J Physiol 589, 4259–4270. 10.1113/jphysiol.2011.208082. [PubMed: 21727221]

Marty VN, Spigelman I, 2012 Long-lasting alterations in membrane properties, k(+) currents, and glutamatergic synaptic currents of nucleus accumbens medium spiny neurons in a rat model of alcohol dependence. Front Neurosci 6, 86 10.3389/fnins.2012.00086. [PubMed: 22701402]

Melnick I, Pronchuk N, Cowley MA, Grove KL, Colmers WF, 2007 Developmental switch in neuropeptide Y and melanocortin effects in the paraventricular nucleus of the hypothalamus. Neuron 56, 1103–1115. 10.1016/j.neuron.2007.10.034. [PubMed: 18093530]

Miyakawa T, Yagi T, Kitazawa H, Yasuda M, Kawai N, Tsuboi K, Niki H, 1997 Fynkinase as a determinant of ethanol sensitivity: relation to NMDA-receptor function. Science 278, 698–701. 10.1126/science.278.5338.698. [PubMed: 9381182]

Morishita W, Marie H, Malenka RC, 2005 Distinct triggering and expression mechanisms underlie LTD of AMPA and NMDA synaptic responses. Nat Neurosci 8, 1043–1050. 10.1038/nn1506. [PubMed: 16025109]

Mönnikes H, Heymann-Mönnikes I, Taché Y, 1992 CRF in the paraventricular nucleus of the hypothalamus induces dose-related behavioral profile in rats. Brain Res 574, 70–76. 10.1016/0006-8993(92)90801-f. [PubMed: 1638411]

Nie Z, Schweitzer P, Roberts AJ, Madamba SG, Moore SD, Siggins GR, 2004 Ethanol augments GABAergic transmission in the central amygdala via CRF1 receptors. Science 303,

Nijholt I, Blank T, Liu A, Kügler H, Spiess J, 2000 Modulation of hypothalamic NMDA receptor function by cyclic AMP-dependent protein kinase and phosphatases. J Neurochem 75, 749–754. 10.1046/j.1471-4159.2000.0750749.x. [PubMed: 10899951]

Ogilvie KM, Lee S, Rivier C, 1997 Role of arginine vasopressin and corticotropin-releasing factor in mediating alcohol-induced adrenocorticotropin and vasopressin secretion in male rats bearing lesions of the paraventricular nuclei. Brain Res 744, 83–95. 10.1016/S0006-8993(96)01082-7. [PubMed: 9030416]

Overstreet DH, Knapp DJ, Breese GR, 2002 Accentuated decrease in social interaction in rats subjected to repeated ethanol withdrawals. Alcohol Clin Exp Res 26, 1259–1268. 10.1097/01.alc.0000023983.10615.d7. [PubMed: 12198403]

Overstreet DH, Knapp DJ, Breese GR, 2004 Modulation of multiple ethanol withdrawal-induced anxiety-like behavior by CRF and CRF1 receptors. Pharmacol Biochem Behav 77, 405–413. 10.1016/j.pbb.2003.11.010. [PubMed: 14751471]

Parkes D, Rivest S, Lee S, Rivier C, Vale W, 1993 Corticotropin-releasing factor activates c-fos, NGFI-B, and corticotropin-releasing factor gene expression within the paraventricular nucleus of the rat hypothalamus. Mol Endocrinol 7, 1357–1367. 10.1210/mend.7.10.8264665. [PubMed: 8264665]

Paxinos G, Watson C, 2009 The Rat Brain in Stereotaxic Coordinates. Sixth ed. London, UK: Academic Press.

Pechnick RN, George R, Poland RE, 1989 Characterization of the effects of the acute and repeated administration of MK-801 on the release of adrenocorticotropin, corticosterone and prolactin in the rat. Eur J Pharmacol 164, 257–263. [PubMed: 2547636]

Pitman DL, Ottenweller JE, Natelson BH, 1988 Plasma corticosterone levels during repeated presentation of two intensities of restraint stress: chronic stress and habituation. Physiol Behav 43, 47–55. 10.1016/0031-9384(88)90097-2. [PubMed: 3413250]

Pohorecky LA, 1991 Stress and alcohol interaction: an update of human research. Alcohol Clin Exp Res 15, 438–459. 10.1111/j.1530-0277.1991.tb00543.x. [PubMed: 1898494]

Rabasa C, Delgado-Morales R, Muñoz-Abellán C, Nadal R, Armario A, 2011 Adaptation of the hypothalamic-pituitary-adrenal axis and glucose to repeated immobilization or restraint stress is not influenced by associative signals. Behav Brain Res 217, 232–239. 10.1016/j.bbr.2010.10.001. [PubMed: 20937327]

Ramot A, Jiang Z, Tian JB, Nahum T, Kuperman Y, Justice N, Chen A, 2017 Hypothalamic CRFR1 is essential for HPA axis regulation following chronic stress. Nat Neurosci 20, 385–388. 10.1038/nn.4491. [PubMed: 28135239]

Ren H, Zhao Y, Dwyer DS, Peoples RW, 2012 Interactions among positions in the third and fourth membrane-associated domains at the intersubunit interface of the N-methyl-D-aspartate receptor forming sites of alcohol action. J Biol Chem 287, 27302–27312. 10.1074/jbc.M111.338921. [PubMed: 22715100]

Richardson HN, Lee SY, O'Dell LE, Koob GF, Rivier CL, 2008 Alcohol self-administration acutely stimulates the hypothalamic-pituitary-adrenal axis, but alcohol dependence leads to a dampened neuroendocrine state. Eur J Neurosci 28, 1641–1653. 10.1111/j.1460-9568.2008.06455.x. [PubMed: 18979677]

Rimondini R, Arlinde C, Sommer W, Heilig M, 2002 Long-lasting increase in voluntary ethanol consumption and transcriptional regulation in the rat brain after intermittent exposure to alcohol. FASEB J 16, 27–35. 10.1096/fj.01-0593com. [PubMed: 11772933]

Rivest S, Rivier C, 1994 Lesions of hypothalamic PVN partially attenuate stimulatory action of alcohol on ACTH secretion in rats. Am J Physiol 266, R553–558. 10.1152/ajpregu.1994.266.2.R553. [PubMed: 8141414]

Rivier C, 2014 Role of hypothalamic corticotropin-releasing factor in mediating alcohol-induced activation of the rat hypothalamic-pituitary-adrenal axis. Front Neuroendocrinol 35, 221–233. 10.1016/j.yfrne.2013.10.005. [PubMed: 24211830]

Rivier C, Bruhn T, Vale W, 1984 Effect of ethanol on the hypothalamic-pituitary-adrenal axis in the rat: role of corticotropin-releasing factor (CRF). J Pharmacol Exp Ther 229, 127–131. [PubMed: 6323684]

Rivier C, Vale W, 1987 Diminished responsiveness of the hypothalamic-pituitary-adrenal axis of the rat during exposure to prolonged stress: a pituitary-mediated mechanism. Endocrinology 121, 1320–1328. 10.1210/endo-121-4-1320. [PubMed: 3498626]

Roberto M, Cruz MT, Gilpin NW, Sabino V, Schweitzer P, Bajo M, Cottone P, Madamba SG, Stouffer DG, Zorrilla EP, Koob GF, Siggins GR, Parsons LH, 2010 Corticotropin releasing factor-induced amygdala gamma-aminobutyric Acid release plays a key role in alcohol dependence. Biol Psychiatry 67, 831–839. 10.1016/j.biopsych.2009.11.007. [PubMed: 20060104]

Roberto M, Madamba SG, Stouffer DG, Parsons LH, Siggins GR, 2004a Increased GABA release in the central amygdala of ethanol-dependent rats. J Neurosci 24, 10159–10166. 10.1523/jneurosci.3004-04.2004. [PubMed: 15537886]

Roberto M, Schweitzer P, Madamba SG, Stouffer DG, Parsons LH, Siggins GR, 2004b Acute and chronic ethanol alter glutamatergic transmission in rat central amygdala: an in vitro and in vivo analysis. J Neurosci 24, 1594–1603. 10.1523/jneurosci.5077-03.2004. [PubMed: 14973247]

Sachs BD, 1988 The development of grooming and its expression in adult animals. Ann N Y Acad Sci 525, 1–17. 10.1111/j.1749-6632.1988.tb38591.x.

Sarkar J, Wakefield S, MacKenzie G, Moss SJ, Maguire J, 2011 Neurosteroidogenesis is required for the physiological response to stress: role of neurosteroid-sensitive GABAA receptors. J Neurosci 31, 18198–18210. 10.1523/jneurosci.2560-11.2011. [PubMed: 22171026]

Schmittgen TD, Livak KJ, 2008 Analyzing real-time PCR data by the comparative C(T) method. Nat Protoc 3, 1101–1108. 10.1038/nprot.2008.73. [PubMed: 18546601]

Sheng H, Zhang Y, Sun J, Gao L, Ma B, Lu J, Ni X, 2008 Corticotropin-releasing hormone (CRH) depresses n-methyl-D-aspartate receptor-mediated current in cultured rat hippocampal neurons via CRH receptor type 1. Endocrinology 149, 1389–1398. 10.1210/en.2007-1378. [PubMed: 18079206]

Siemsen BM, Lombroso PJ, McGinty JF, 2018 Intra-prelimbic cortical inhibition of striatal-enriched tyrosine phosphatase suppresses cocaine seeking in rats. Addict Biol 23, 219–229. 10.1111/adb.12504. [PubMed: 28349660]

Silberman Y, Fetterly TL, Awad EK, Milano EJ, Usdin TB, Winder DG, 2015 Ethanol produces corticotropin-releasing factor receptor-dependent enhancement of spontaneous glutamatergic transmission in the mouse central amygdala. Alcohol Clin Exp Res 39, 2154–2162. 10.1111/acer.12881. [PubMed: 26503065]

Simmons DM, Swanson LW, 2009 Comparison of the spatial distribution of seven types of neuroendocrine neurons in the rat paraventricular nucleus: toward a global 3D model. J Comp Neurol 516, 423–441. 10.1002/cne.22126. [PubMed: 19655400]

Simms JA, Nielsen CK, Li R, Bartlett SE, 2014 Intermittent access ethanol consumption dysregulates CRF function in the hypothalamus and is attenuated by the CRF-R1 antagonist, CP-376395. Addict Biol 19, 606–611. 10.1111/adb.12024. [PubMed: 23362976]

Sinha R, Fox HC, Hong KA, Bergquist K, Bhagwagar Z, Siedlarz KM, 2009 Enhanced negative emotion and alcohol craving, and altered physiological responses following stress and cue exposure in alcohol dependent individuals. Neuropsychopharmacology 34, 1198–1208. 10.1038/npp.2008.78. [PubMed: 18563062]

Sinha R, Fox HC, Hong KI, Hansen J, Tuit K, Kreek MJ, 2011 Effects of adrenal sensitivity, stress- and cue-induced craving, and anxiety on subsequent alcohol relapse and treatment outcomes. Arch Gen Psychiatry 68, 942–952. 10.1001/archgenpsychiatry.2011.49. [PubMed: 21536969]

Smothers CT, Woodward JJ, 2016 Differential effects of TM4 tryptophan mutations on inhibition of N-methyl-d-aspartate receptors by ethanol and toluene. Alcohol 56, 15–19. 10.1016/j.alcohol.2016.10.001. [PubMed: 27814790]

Sommer WH, Rimondini R, Hansson AC, Hipskind PA, Gehlert DR, Barr CS, Heilig MA, 2008 Upregulation of voluntary alcohol intake, behavioral sensitivity to stress, and amygdala crhr1 expression following a history of dependence. Biol Psychiatry 63, 139–145. 10.1016/j.biopsych.2007.01.010. [PubMed: 17585886]

Sparta DR, Hopf FW, Gibb SL, Cho SL, Stuber GD, Messing RO, Ron D, Bonci A, 2013 Binge ethanol-drinking potentiates corticotropin releasing factor R1 receptor activity in the ventral tegmental area. Alcohol Clin Exp Res 37, 1680–1687. 10.1111/acer.12153. [PubMed: 23763790]

Spruijt BM, van Hooff JA, Gispen WH, 1992 Ethology and neurobiology of grooming behavior. Physiol Rev 72, 825–852. 10.1152/physrev.1992.72.3.825. [PubMed: 1320764]

Sterley TL, Baimoukhametova D, Füzesi T, Zurek AA, Daviu N, Rasiah NP, Rosenegger D, Bains JS, 2018 Social transmission and buffering of synaptic changes after stress. Nat Neurosci 21, 393–403. 10.1038/s41593-017-0044-6. [PubMed: 29311741]

Stern JE, 2001 Electrophysiological and morphological properties of pre-autonomic neurones in the rat hypothalamic paraventricular nucleus. J Physiol 537, 161–177. 10.1111/j.1469-7793.2001.0161k.x. [PubMed: 11711570]

Ungless MA, Singh V, Crowder TL, Yaka R, Ron D, Bonci A, 2003 Corticotropin-releasing factor requires CRF binding protein to potentiate NMDA receptors via CRF receptor 2 in dopamine neurons. Neuron 39, 401–407. 10.1016/S0896-6273(03)00461-6. [PubMed: 12895416]

Vahl TP, Ulrich-Lai YM, Ostrander MM, Dolgas CM, Elfers EE, Seeley RJ, D'Alessio DA, Herman JP, 2005 Comparative analysis of ACTH and corticosterone sampling methods in rats. Am J Physiol Endocrinol Metab 289, E823–828. 10.1152/ajpendo.00122.2005. [PubMed: 15956051]

Valdez GR, Roberts AJ, Chan K, Davis H, Brennan M, Zorrilla EP, Koob GF, 2002 Increased ethanol self-administration and anxiety-like behavior during acute ethanol withdrawal and protracted abstinence: regulation by corticotropin-releasing factor. Alcohol Clin Exp Res 26, 1494–1501. 10.1097/01.alc.0000033120.51856.f0. [PubMed: 12394282]

Valdez GR, Zorrilla EP, Roberts AJ, Koob GF, 2003 Antagonism of corticotropin-releasing factor attenuates the enhanced responsiveness to stress observed during protracted ethanol abstinence. Alcohol 29, 55–60. 10.1016/s0741-8329(03)00020-x. [PubMed: 12782246]

Van Erp AM, Kruk MR, Meelis W, Willekens-Bramer DC, 1994 Effect of environmental stressors on time course, variability and form of self-grooming in the rat: handling, social contact, defeat,

novelty, restraint and fur moistening. Behav Brain Res 65, 47–55. 10.1016/0166-4328(94)90072-8. [PubMed: 7880454]

Van Erp AM, Kruk MR, Willekens-Bramer DC, Bressers WM, Roeling TA, Veening JG, Spruyt BM, 1991 Grooming induced by intrahypothalamic injection of ACTH in the rat: comparison with grooming induced by intrahypothalamic electrical stimulation and i.c.v. injection of ACTH. Brain Res 538, 203–210. 10.1016/0006-8993(91)90431-t. [PubMed: 1849437]

Vogel C, Marcotte EM, 2012 Insights into the regulation of protein abundance from proteomic and transcriptomic analyses. Nat Rev Genet 13, 227–232. 10.1038/nrg3185. [PubMed: 22411467]

Wamsteeker Cusulin JI, Fuzesi T, Inoue W, Bains JS, 2013a Glucocorticoid feedback uncovers retrograde opioid signaling at hypothalamic synapses. Nat Neurosci 16, 596–604. 10.1038/nn.3374. [PubMed: 23563581]

Wamsteeker Cusulin JI, Füzesi T, Watts AG, Bains JS, 2013b Characterization of corticotropin-releasing hormone neurons in the paraventricular nucleus of the hypothalamus of Crh-IRES-Cre mutant mice. PLoS One 8, e64943 10.1371/journal.pone.0064943. [PubMed: 23724107]

Wamsteeker JI, Kuzmiski JB, Bains JS, 2010 Repeated stress impairs endocannabinoid signaling in the paraventricular nucleus of the hypothalamus. J Neurosci 30, 11188–11196. 10.1523/jneurosci.1046-10.2010. [PubMed: 20720126]

Wang J, Lanfranco MF, Gibb SL, Yowell QV, Carnicella S, Ron D, 2010 Long-lasting adaptations of the NR2B-containing NMDA receptors in the dorsomedial striatum play a crucial role in alcohol consumption and relapse. J Neurosci 30, 10187–10198. 10.1523/jneurosci.2268-10.2010. [PubMed: 20668202]

Wang LY, Orser BA, Brautigan DL, MacDonald JF, 1994 Regulation of NMDA receptors in cultured hippocampal neurons by protein phosphatases 1 and 2A. Nature 369, 230–232. 10.1038/369230a0. [PubMed: 8183343]

Wang YT, Salter MW, 1994 Regulation of NMDA receptors by tyrosine kinases and phosphatases. Nature 369, 233–235. 10.1038/369233a0. [PubMed: 7514272]

Westphal RS, Tavalin SJ, Lin JW, Alto NM, Fraser ID, Langeberg LK, Sheng M, Scott JD, 1999 Regulation of NMDA receptors by an associated phosphatase-kinase signaling complex. Science 285, 93–96. 10.1126/science.285.5424.93. [PubMed: 10390370]

Whitnall MH, Mezey E, Gainer H, 1985 Co-localization of corticotropin-releasing factor and vasopressin in median eminence neurosecretory vesicles. Nature 317, 248–250. 10.1038/317248a0. [PubMed: 3900740]

Wiegant VM, Jolles J, Colbern DL, Zimmermann E, Gispen WH, 1979 Intracerebroventricular ACTH activates the pituitary-adrenal system:dissociation from a behavioral response. Life Sci 25, 1791–1796. 10.1016/0024-3205(79)90425-9. [PubMed: 231165]

Wright JM, Peoples RW, Weight FF, 1996 Single-channel and whole-cell analysis of ethanol inhibition of NMDA-activated currents in cultured mouse cortical and hippocampal neurons. Brain Res 738, 249–256. 10.1016/S0006-8993(96)00780-9. [PubMed: 8955520]

Wu PH, Coultrap S, Browning MD, Proctor WR, 2010 Correlated changes in NMDA receptor phosphorylation, functional activity, and sedation by chronic ethanol consumption. J Neurochem 115, 1112–1122. 10.1111/j.1471-4159.2010.06991.x. [PubMed: 20831600]

Zhao Y, Ren H, Dwyer DS, Peoples RW, 2015 Different sites of alcohol action in the NMDA receptor GluN2A and GluN2B subunits. Neuropharmacology 97, 240–250. 10.1016/j.neuropharm.2015.05.018. [PubMed: 26051400]

Zhou Y, Yuferov VP, Spangler R, Maggos CE, Ho A, Kreek MJ, 1998 Effects of memantine alone and with acute ‘binge’ cocaine on hypothalamic-pituitary-adrenal activity in the rat. Eur J Pharmacol 352, 65–71. 10.1016/S0014-2999(98)00332-x. [PubMed: 9718269]

Zorrilla EP, Valdez GR, Weiss F, 2001 Changes in levels of regional CRF-like-immunoreactivity and plasma corticosterone during protracted drug withdrawal in dependent rats. Psychopharmacology (Berl) 158, 374–381. 10.1007/s002130100773. [PubMed: 11797058]

Highlights

- Chronic intermittent ethanol alters parvocellular neurosecretory cell excitability.
- CIE increases GluN2B subunit-dependent NMDAR function in PNCs.
- CIE prevents CRF- and ethanol-induced decreases in NMDAR currents of PNCs.
- CIE prevents stress-induced synaptic plasticity at PNC glutamatergic synapses.
- CIE dysregulates stress-induced HPA axis hormonal and behavioral responses.

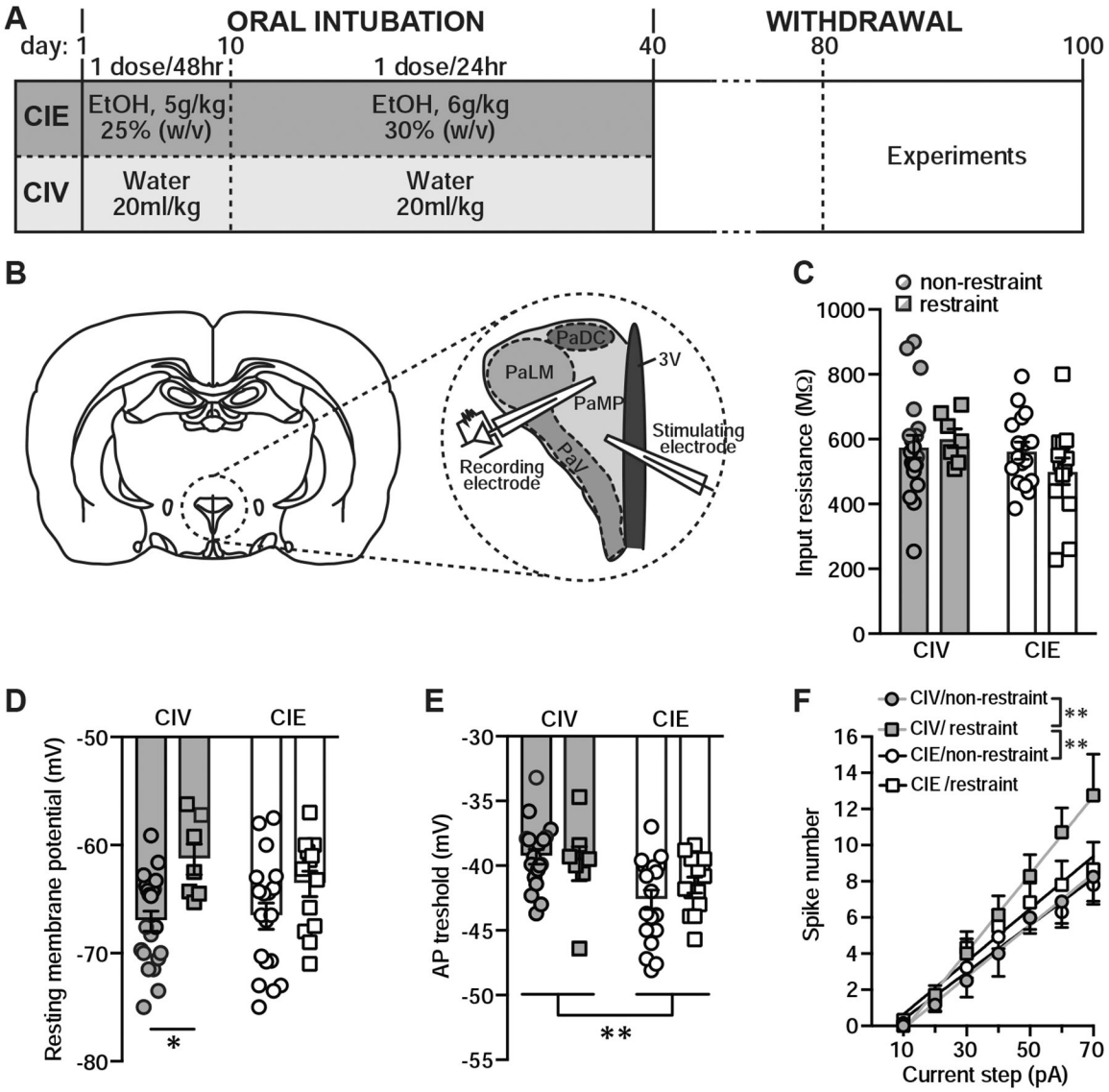

Figure 1.

Stress and CIE alter PNC membrane properties. **A**, Representation of the experimental design used in the CIV and CIE group. **B**, Schematic diagram of coronal brain slice illustrating the location of stimulating and recording electrodes in the expanded view. PNCs were recorded from the dorsal zone of the medial parvocellular part of the PVN (PaMP). Adapted from Paxinos & Watson (2009) and reproduced from Marty et al. (2011) with permission. **C**, Summary graph showing individual (circles/squares) and averaged (bars) input resistance of PNCs from CIV and CIE rats with or without restraint. **D**, Summary graph showing RMP of PNCs. **E**, Summary graph showing reduced AP threshold in PNCs of CIE rats. **F**, Summary graph showing the input-output curve.

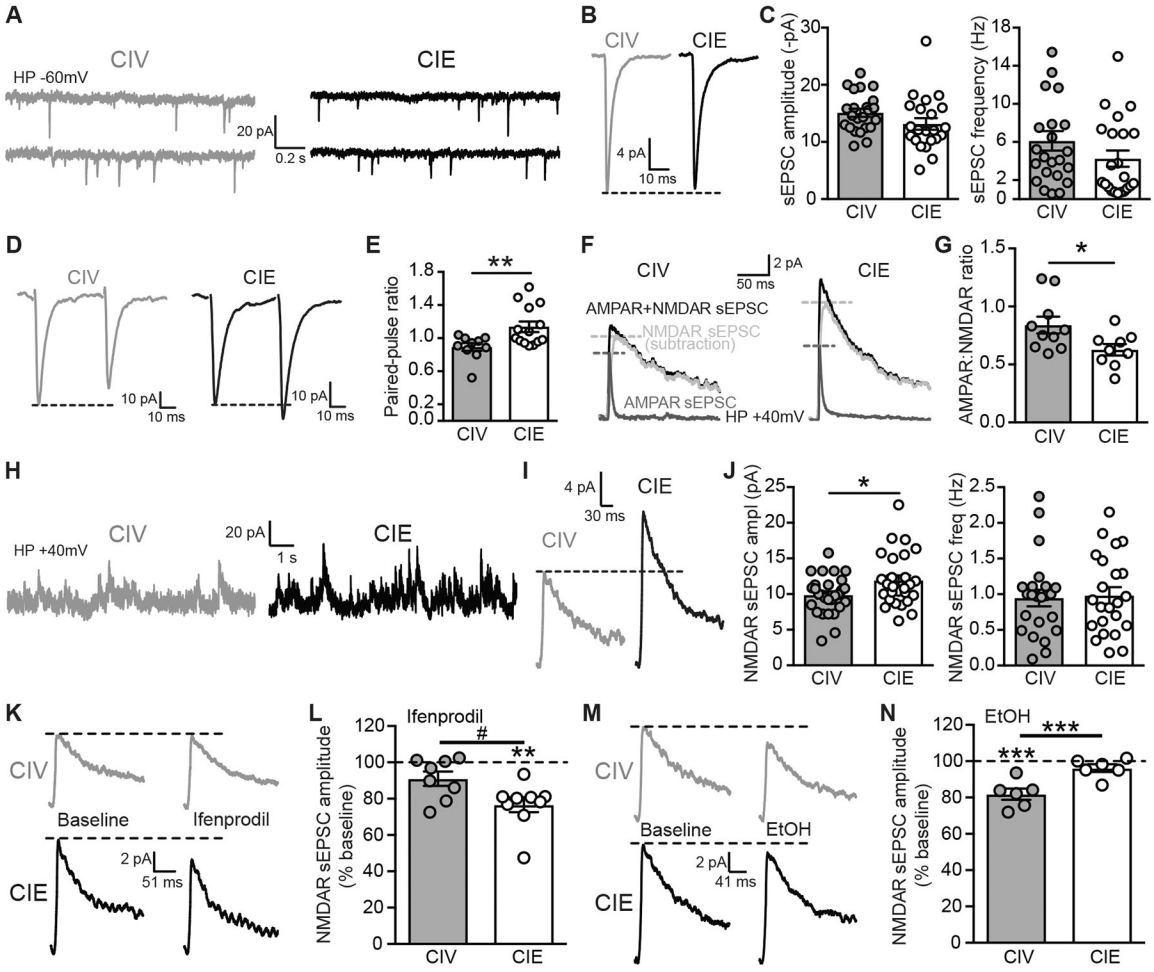

Figure 2.

CIE increases NR2B subunit-dependent NMDAR function. Representative traces (**A**) and averaged (**B**) AMPAR-mediated sEPSCs recorded at a holding potential of −60 mV of one PNC from CIV (left, top and bottom grey traces) and one PNC from CIE (right, top and bottom black traces) rats. The bottom trace is a continuation of the top trace. **C**, Summary graphs of average (and individual) AMPAR-sEPSC amplitude (left) and frequency (right) of PNCs from CIV and CIE rats. **D**, Representative averaged AMPAR-mediated eEPSCs elicited by two stimuli (25ms interval) used to calculate the paired-pulse ratio (PPR) of PNCs from CIV (left, grey) and CIE (right, black) rats. **E**, Summary graph of significantly increased PPR in PNCs of CIE rats. **F**, Representative averaged traces of AMPAR +NMDAR-mediated sEPSCs (black), AMPAR-sEPSC (dark grey) and NMDAR-sEPSC (subtraction of AMPAR-sEPSC from AMPAR+NMDAR-sEPSC; light grey) recorded at a holding potential of +40mV of PNCs from CIV (left) and CIE (right) rats. **G**, Summary graph of significant increases in AMPAR:NMDAR ratio in PNCs of CIE rats compared to CIV. The NMDAR antagonist APV (40 μM; Abcam) was applied to isolate the AMPAR-mediated sEPSCs at +40 mV. Representative traces (**H**) and averaged (**I**) NMDAR-mediated sEPSCs recorded at a holding potential of +40 mV of PNCs from CIV (left, grey) and CIE (right, black) rats. **J**, Summary graph showing the increase in NMDAR-sEPSC amplitude

(left), but not frequency (right), in CIE. **K**, Representative averaged NMDAR-sEPSCs before and after ifenprodil (5 μM) in CIV (top) and CIE (bottom). **L**, Summary graph showing ifenprodil-induced decrease in NMDAR-sEPSC amplitude in CIE. **p<0.01, Wilcoxon paired-test, baseline vs. ifenprodil in CIE; #p<0.05, % inhibition CIV vs. CIE. Representative averaged (**M**) and summary graph (**N**) showing EtOH-induced decreases in NMDAR-sEPSC amplitude in CIV but not CIE.

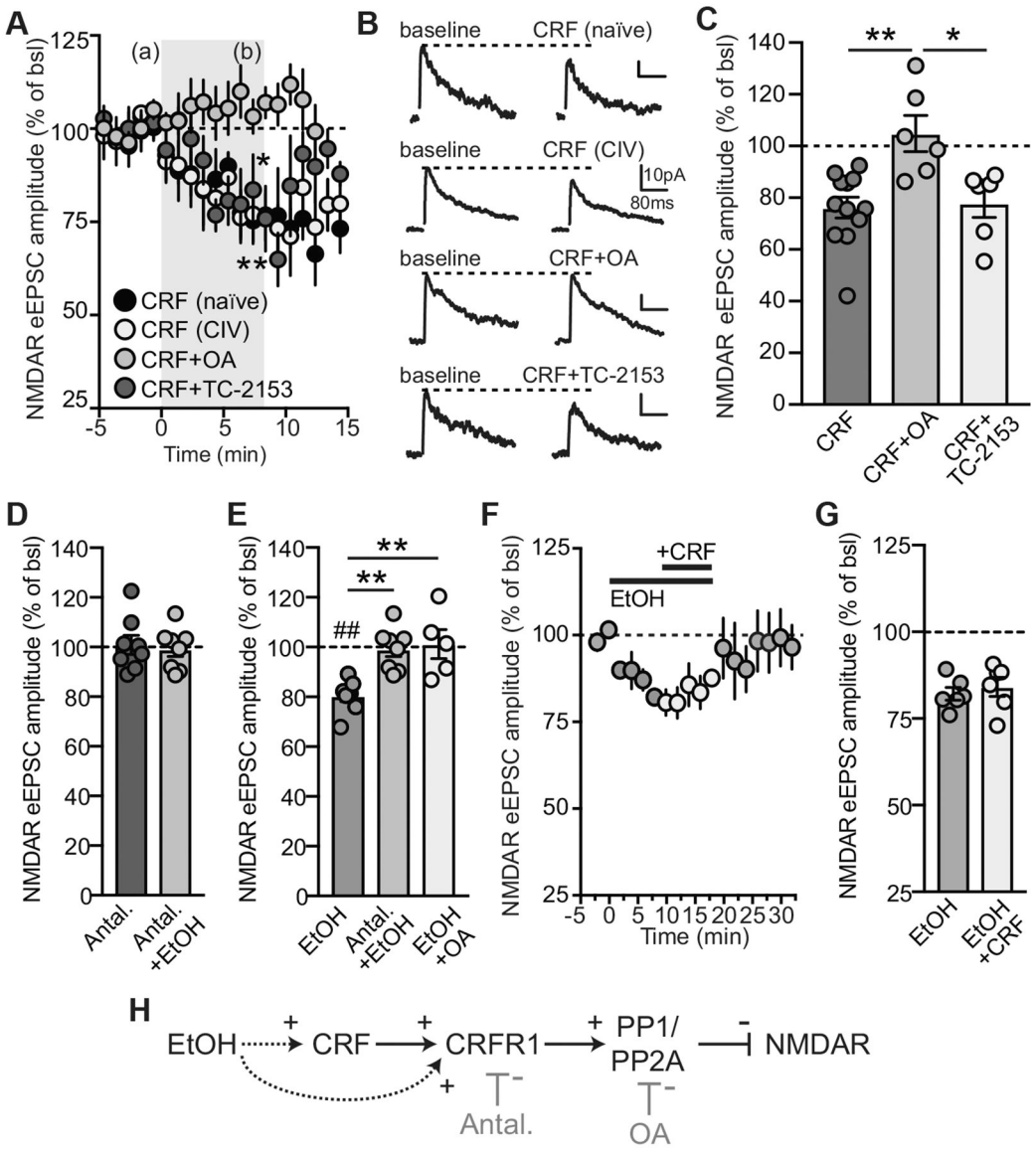

Figure 3.

CRF and EtOH inhibition of NMDAR-currents share similar intracellular mechanisms involving phosphatase activation in control rats. **A**, Summary time course showing that CRF (1 μM) decreases NMDAR-eEPSC amplitude in PNCs from naïve and CIV rats. Addition in the internal solution of okadaic acid (OA, 1 μM), but not TC-2153 (1μM), prevents CRF-induced decreases in NMDAR currents in PNCs from naïve rats. Time of drug application is represented by the grey shadow. EPSCs were evoked every 15 sec. Drug effect was calculated as the average amplitude of 8 eEPSCs during baseline and at 7–8 min during drug bath application. **B**, Representative averaged NMDAR-eEPSCs before and after CRF (top), CRF+OA (lower middle), and CRF+TC-2153 (bottom) in naïve and CIV (upper top) rats. **C**, Summary graph of OA effects on CRF-induced decreases in NMDAR function. **D**, Summary graph showing the lack of effect of ethanol on NMDAR-eEPSC amplitude in the presence of antalarmin. Antalarmin alone did not affect NMDAR-eEPSCs, but prevented ethanol-

induced decreases in NMDAR-eEPSC amplitude. **E**, Summary graph of antalarmin (Antal.+EtOH, n=8/N=7) and OA (EtOH+OA, n=5/N=4) effects on EtOH-induced decreases in NMDAR function. **p<0.01, one-way ANOVA, Tukey's post hoc; ##p<0.01, paired t-test, baseline vs. ethanol. **F**, Summary time course showing the occlusion between EtOH (100 mM) and CRF (1 μM) in inhibiting NMDAR currents. **G**, Summary graph showing the inhibitory effects of EtOH alone and with CRF. **H**: Schematic representing the putative molecular mechanisms involved in CRF- and ethanol-induced NMDAR inhibition.

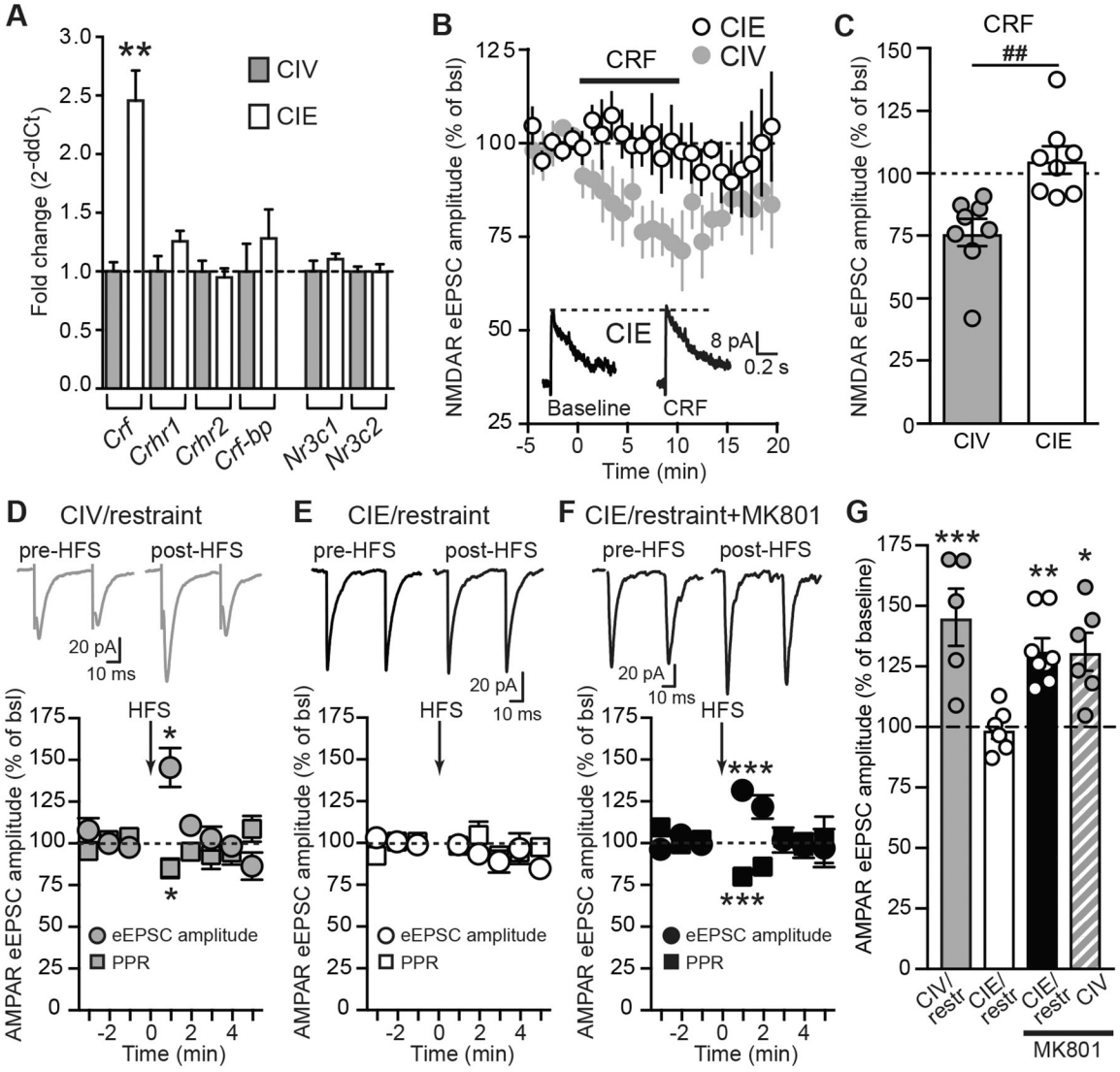

Figure 4.

CIE exposure alters CRF expression in the PVN, prevents CRF- and EtOH-induced decreases in NMDAR-currents, and synaptic plasticity of AMPAR-currents in PVN PNCs. **A**, Summary graph showing the fold change (2^{-ddCT}) of mRNA expression of *Crf*, *Crhr1*, *Crhr2*, *Crf-bp*, *Nr3c1*, and *Nr3c2* in CIE compared to CIV rats. The fold change in gene expression between CIV and CIE groups was calculated as 2^{-ddCT} (with $ddC_T=dC_T[CIE] - dC_T[CIV]$). **B**, Summary time course showing that CIE exposure prevents CRF-induced decreases in NMDAR eEPSC amplitude in PNCs. Summary CIV time course as shown in Fig. 3A. **C**, Summary graph showing the significant inhibitory effects of CRF in CIV but not in CIE rats. CRF data in bar graph for CIV are duplicate from Fig. 3C. **D**, Top, representative traces of paired-pulse AMPAR-eEPSCs recorded from PNCs, evoked pre-HFS and post-HFS in slices from CIV/restraint rats. Bottom, summary time course of AMPAR-eEPSC amplitude and PPR pre- and post-HFS. HFS induces a significant increase in eEPSC amplitude and decrease in PPR. EPSC were evoked every 5 sec. The magnitude of STP was calculated as the average amplitude of 12 eEPSCs immediately following HFS (0–

1 min post-HFS) and was expressed as % of baseline. **E**, Top, representative traces of paired-pulse AMPAR-eEPSCs recorded from PNCs, evoked pre-HFS and post-HFS in slices from CIE/restraint rats. Bottom, summary time course of AMPAR-eEPSC amplitude and PPR pre- and post-HFS. HFS-induced STP is impaired in CIE/restraint rats. **F**, Top, representative traces of paired-pulse AMPAR-eEPSCs recorded from PNCs, evoked pre-HFS and post-HFS in slices from CIE/restraint rats with MK801 (1 mM) included in intrapipette solution. Bottom, NMDAR inhibition with MK801 rescues HFS-induced STP associated with decreased PPR in PNCs from CIE/restraint rats. **G**, Summary bar graph showing that stress and inhibition of postsynaptic NMDARs unmask synaptic plasticity in CIV rats (CIV/restraint, grey bar; CIV/non-restraint+MK801, grey hatched bar). While CIE exposure prevents stress-induced synaptic plasticity, inhibition of NMDARs rescues STP (CIE/restraint, white bar; CIE/restraint+MK801, black bar).

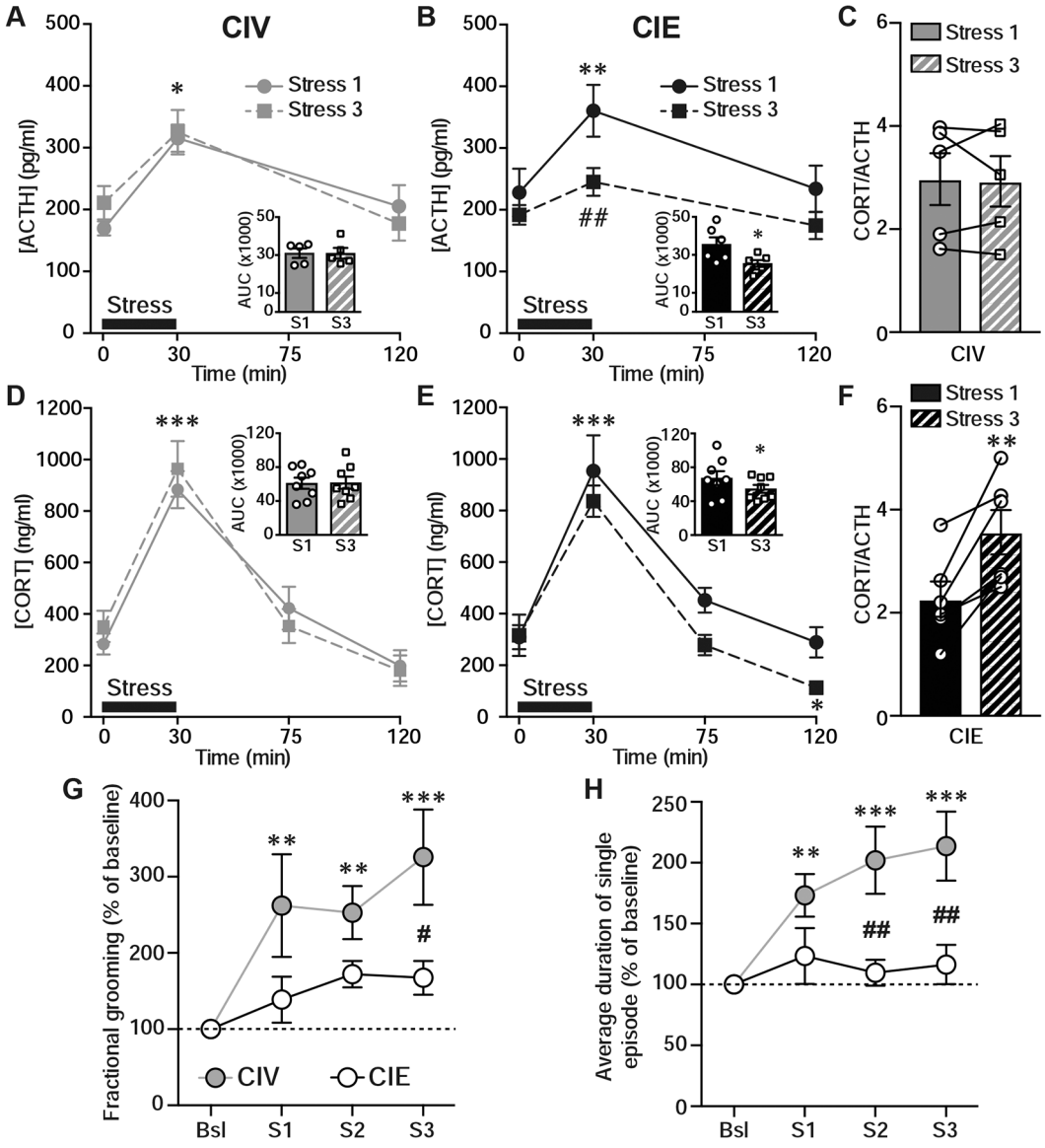

Figure 5.

CIE reduces HPA axis hormonal responses and self-grooming responses to repeated restraint stress. **A-B**, Plasma ACTH levels in response to the restraint stress at t=0, 30, and 120 min post-stress in CIV (A) and CIE rats (B). Insert, integrated ACTH response, represented as area under the curve (AUC), to stress 1 (S1) and stress 3 (S3) in CIV (A) and CIE (B) rats. CIE significantly blunted ACTH response to stress 3. **C**, Summary graph of CORT/ACTH ratio at t=30 min post-stress 1 and stress 3 in CIV. **D-E**, Plasma CORT levels in response to restraint stress at t=0, 30, 75 and 120 min post-stress in CIV (D) and CIE (E) rats. Insert, integrated CORT response to S1 and S3 in CIV (D) and CIE (E) rats. CIE significantly reduced CORT response to stress 3. **F**, Summary graph of CORT/ACTH ratio at t=30 min post-stress 1 and stress 3 in CIE rats. CIE significantly increased CORT/ACTH in response to stress 3 compared to stress 1. **G**, Fractional time grooming, defined as the relative time spent grooming during the exploring time period, was significantly increased following

stress in CIV rats, these increases were blunted in CIE rats. **p<0.01, ***p<0.001, baseline vs. stress; #p<0.05, CIV vs. CIE. **H**, CIE blunts stress-induced increases in average duration of a single grooming episode, expressed as % of baseline. **p<0.01, ***p<0.001, baseline vs. stress; ##p<0.01, CIV vs. CIE.